

# 1 Water droplet-in-oil digestion method for single-cell proteomics

2  
3 Takeshi Masuda<sup>1,2,\*</sup>, Yuma Inamori<sup>2</sup>, Arisu Furukawa<sup>2</sup>, Kazuki Momosaki<sup>3</sup>, Chih-  
4 Hsiang Chang<sup>4</sup>, Daiki Kobayashi<sup>4,5</sup>, Hiroto Ohguchi<sup>6</sup>, Yawara Kawano<sup>7</sup>, Shingo Ito<sup>1,2</sup>,  
5 Norie Araki<sup>4</sup>, Shao-En Ong<sup>8</sup>, Sumio Ohtsuki<sup>1,2</sup>

6  
7 **Affiliations**

8 <sup>1</sup> Department of Pharmaceutical Microbiology, Faculty of Life Sciences, Kumamoto  
9 University, Kumamoto, Japan

10 <sup>2</sup> Department of Pharmaceutical Microbiology, Graduate School of Pharmaceutical  
11 Sciences, Kumamoto University, Kumamoto, Japan

12 <sup>3</sup> Department of Pharmaceutical Microbiology, School of Pharmacy, Kumamoto  
13 University, Kumamoto, Japan

14 <sup>4</sup> Department of Tumor Genetics and Biology, Graduate School of Medical Sciences,  
15 Kumamoto University, Kumamoto, Japan

16 <sup>5</sup> Department of Omics Biology, Graduate School of Medical and Dental Sciences,  
17 Niigata University, Niigata, Japan

18 <sup>6</sup> Division of Disease Epigenetics, Institute of Resource Development and Analysis,  
19 Kumamoto University, Kumamoto, Japan

20 <sup>7</sup> Department of Hematology, Rheumatology, and Infectious Diseases, Faculty of Life  
21 Sciences, Kumamoto University, Kumamoto, Japan

22 <sup>8</sup> University of Washington, Department of Pharmacology, Seattle, WA USA

23  
24 **\*Corresponding author: Takeshi Masuda, Ph.D.**

25 Department of Pharmaceutical Microbiology, Faculty of Life Sciences, Kumamoto  
26 University, 5-1 Oe-honmachi, Chuo-ku, Kumamoto 862-0973, Japan

27 TEL: +81-96-371-4329; FAX: +81-96-371-4329; E-mail: tmasuda@kumamoto-u.ac.jp

30 **Abstract**

31 Recent advances in single-cell proteomics highlight the promise of sensitive analyses  
32 in limited cell populations. However, technical challenges remain for sample recovery,  
33 throughput, and versatility. Here, we first report a water droplet-in-oil digestion  
34 (WinO) method based on carboxyl-coated beads and phase transfer surfactants for  
35 proteomic analysis using limited sample amounts. This method was developed to  
36 minimize the contact area between the sample solution and the container to reduce  
37 the loss of proteins and peptides by adsorption. This method increased protein and  
38 peptide recovery 10-fold as well as the number of quantified transmembrane proteins  
39 compared to an in-solution digestion (ISD) method. The proteome profiles obtained  
40 from 100 cells using the WinO method highly correlated with those from 10000 cells  
41 using the ISD method. We successfully applied the WinO method to single-cell  
42 proteomics and quantified 462 proteins. Using the WinO method, samples can be  
43 easily prepared in a multi-well plate, making it a widely applicable and suitable  
44 method for single-cell proteomics.

45

46 **Keywords**

47 Single-cell, Proteomics, Water droplet-in oil, Cell sorter, Carboxyl-coated beads

48

49 **Introduction**

50 In recent decades, single-cell omics has become an important analytical technique in  
51 several research fields that has brought new perspectives to cancer genomics<sup>1-3</sup>,  
52 tissue development<sup>4</sup>, and cellular differentiation<sup>5-8</sup>. The genome and transcriptome  
53 are currently the main targets of single-cell omics studies. Quantitative  
54 amplification and next-generation sequencing enable high-throughput single-cell  
55 epigenetic and transcriptional analyses. Proteins are important biomolecules  
56 playing a major role in biological phenomena. Furthermore, because protein  
57 expression levels are reportedly difficult to predict based solely on mRNA expression  
58 levels<sup>9,10</sup>, there remains a need to measure protein expression directly with  
59 proteomics.

60 For single-cell proteomics, high recovery of proteins and peptides, as well as high  
61 throughput, are required. To quantify proteins by proteomics, extracted proteins are  
62 digested into peptides by enzymes and then analyzed by nano-liquid  
63 chromatography-tandem mass spectrometry (nanoLC-MS/MS). Additionally, no  
64 current method can amplify proteins. Hence, it is critical to reduce adsorption losses  
65 during sample preparation and to enhance protein extraction and digestion in single-

66 cell proteomics. Several sample preparation methods, such as single-cell proteomics  
67 by mass spectrometry (SCoPE-MS)<sup>11</sup>, nanodroplet processing in one-pot for trace  
68 samples (nanoPOTS)<sup>12,13</sup>, and surfactant-assisted one-pot sample preparation  
69 coupled with mass spectrometry (SOP-MS)<sup>14</sup>, can dramatically improve the sample  
70 recovery rate and sensitivity of MS for single-cell proteomics. Using these  
71 approaches combined with state-of-the-art LC-MS systems, the number of proteins  
72 identified from single cell was dramatically increased. SCoPE-MS is based on  
73 multiplexing with a tandem mass tag (TMT) reagent where small amounts of  
74 samples are mixed with a carrier containing large amounts of peptides, thus  
75 reducing sample loss during LC injection. In addition, the greater signal intensity of  
76 peptides from the carrier proteome can increase to the number of MS/MS triggers.  
77 However, because the SCoPE-MS uses an in-solution digestion (ISD) method, there  
78 will be loss of proteins and peptides at the stage of sample preparation prior to LC-  
79 MS analyses<sup>11</sup>. The nanoPOTS method uses a specially fabricated nano-well chip and  
80 a liquid handling system for digestion. These devices were designed to process the  
81 sample in a small volume to reduce protein and peptide adsorption loss<sup>12,13</sup>. However,  
82 because these devices are not yet commercially available, and the workflow is tied to  
83 the microfluidic system, the versatility of the nanoPOTS is lower than that of other  
84 approaches. The SOP-MS was developed for label-free single-cell proteomics<sup>14</sup>. This  
85 approach eliminates all sample transfer steps. The sample preparation was  
86 performed in the presence of an MS-compatible surfactant<sup>15</sup>, n-dodecyl- $\beta$ -D-  
87 maltoside, to reduce the adsorption loss of the samples by blocking protein  
88 adsorption on plastic surfaces<sup>14</sup>. The SOP-MS was successfully applied to sorted  
89 single cells and small tissue sections obtained by laser microdissection. However, the  
90 throughput of this approach on the nanoLC-MS/MS is limited due to the lack of a  
91 multiplexing approach. While these advances enable single-cell proteomics,  
92 technical challenges remain for the recovery rate, versatile application, and  
93 increased throughput.

94 Herein, we report a simple and highly efficient sample preparation method for  
95 single-cell proteomics that prepares samples in a water droplet, termed water droplet-  
96 in-oil digestion (WinO). This new method reduces sample loss during single-cell  
97 protein preparations and increases the number of identified proteins compared with  
98 the ISD methods. The WinO method improves current single-cell proteomics  
99 methods and can enhance the throughput and protein identification from single-cell  
100 sampling.

101

102 **Methods**

103 **Reagents and chemicals**

104 Sodium deoxycholate (SDC), sodium lauryl sarcosinate (SLS), ammonium  
105 bicarbonate (AmBic), dithiothreitol (DTT), iodoacetamide (IAA), mass-spectrometry-  
106 grade lysyl endopeptidase (Lys-C), ethyl acetate, acetonitrile, acetic acid,  
107 trifluoroacetic acid (TFA), Dulbecco's modified Eagle medium (DMEM), negative  
108 staining kit, and RPMI-1640 medium were purchased from Fujifilm Wako (Osaka,  
109 Japan). Triethylammonium bicarbonate (TEAB), SOURCE 30S beads, and SP  
110 Sepharose High Performance beads were from Sigma-Aldrich (St. Louis, MO, USA).  
111 Modified trypsin was obtained from Promega (Madison, WI, USA). SDC-XC StageTip  
112 was purchased from GL Sciences (Tokyo, Japan). Carboxyl-coated Magnosphere  
113 beads were obtained from JSR Life Sciences (Tsukuba, Japan). Benzonase nuclease  
114 was purchased from Merck Millipore (Burlington, MA, USA). LDS sample buffer,  
115 BCA assay kit, Tandem Mass Tags reagents, and Dynabeads MyOne Carboxylic acid  
116 were obtained from Thermo Scientific (San Jose, CA, USA). FG beads COOH and FG  
117 beads NH<sub>2</sub> were from TAMAGAWA SEIKI (Nagano, Japan).

118

119 **Cell culture and cell sorting**

120 In this study, 15 multiple myeloma cell lines (H929, KMM-1, KMS-11, KMS-12BM,  
121 KMS-12PE, KMS-20, KMS-27, KMS-28BM, KMS-28PE, L363, MM.1S, MOLP8,  
122 OPM1, RPMI8226, and U266 cells) were cultured in RPMI-1640 medium  
123 supplemented with 10% FCS to 80% confluence. Cells were washed three times with  
124 PBS, and then 1 or 100 cells were sorted into 96-well plates. For 10000 cells, cells  
125 were sorted into 1.5 mL tubes. As a cell sorter, an SH800S Cell Sorter (Sony, Tokyo,  
126 Japan) using a 100-μm chip was used. Dead and doublet cells were removed prior to  
127 cell sorting. HEK293 cell was cultured in DMEM supplemented with 10% FCS to  
128 80% confluence. Cells were harvested by scraper and washed three times with PBS.

129

130 **Examination of proteins and peptides retention in water droplet in ethyl acetate**

131 The protein solution was prepared by extraction from HEK293 cells using the 12 mM  
132 SDC and 12 mM SLS in 100 mM Tris-HCl (pH 9.0). The protein amount was  
133 quantified by the BCA assay kit. To examine protein retention in water droplets in  
134 ethyl acetate, 50 μL of solution containing 10 μg of HEK293 proteins was dropped  
135 into 500 μL of ethyl acetate in a 1.5 mL tube. The samples were incubated for 24  
136 hours at 25 °C. The ethyl acetate and water droplet were transferred by pipette tip  
137 into a new 1.5 mL tube and evaporated with a centrifuge concentrator. Each fraction

138 was reconstituted with 20  $\mu$ L of LDS sample buffer and separated by 5-20% SDS-  
139 PAGE. To prepare the negative control sample, we performed the same process as  
140 described above using the extraction buffer containing 12 mM SDC and 12 mM SLS  
141 in 100 mM Tris-HCl (pH 9.0). As the positive control, 10  $\mu$ g of HEK293 proteins were  
142 separated by SDS-PAGE together. The protein bands in the gel were detected by the  
143 negative staining.

144 To examine the peptide retention in the water droplet in ethyl acetate, the HEK293  
145 peptides prepared by the ISD method were used. To prepare the peptide solution, 10  
146  $\mu$ g of HEK293 proteins were reduced and alkylated with 10 mM DTT and 50 mM  
147 IAA, respectively. The protein solution was diluted 4-fold with 50 mM AmBic prior  
148 to enzymatic digestion. Proteins were digested with 0.5  $\mu$ g of Lys-C followed by 0.5  
149  $\mu$ g of trypsin overnight at 37 °C. For the evaluation, 20  $\mu$ L of solution containing 10  
150  $\mu$ g of HEK293 peptides was dropped into 200  $\mu$ L of ethyl acetate and incubated at 25  
151 °C for 24 hours. The ethyl acetate and water droplet were transferred by pipette tip  
152 into a new 1.5 mL tube and dried with the centrifuge concentrator. Each fraction was  
153 reconstituted by the 50  $\mu$ L of 50 mM AmBic and subjected to the phase transfer  
154 method to remove SDC and SLS. The peptides purified with SDB-XC StageTip were  
155 analyzed by nanoLC-MS/MS using TripleTOF 5600 (Sciex, Framingham, MA). As  
156 the positive control, 10  $\mu$ g of HEK293 peptides purified by SDB-XC StageTip were  
157 used for nanoLC-MS/MS. To prepare the negative control sample, we performed the  
158 same process as described above using the buffer containing 3 mM SDC, 3 mM SLS,  
159 37.5 mM AmBic in 25 mM Tris-HCl (pH 9.0).

160

## 161 **Sample preparation using the ISD method**

162 First, 1  $\mu$ L extraction buffer (50 mM TEAB, 12 mM SDC, 12 mM SLS, and 0.125  
163 units benzonase) was added into low protein-binding 96-well plates (Sumitomo  
164 Bakelite, Tokyo, Japan) or into low protein-binding 1.5 mL tubes (Watson, Tokyo,  
165 Japan). Cells were sorted into each well and spun at 300  $\times g$  for 1 min at 25 °C to  
166 mix the extraction buffer and the cells. The reduction and alkylation were performed  
167 by adding 1  $\mu$ L 100 mM DTT and 550 mM IAA solution, respectively. The DTT and  
168 IAA solutions were prepared by 50 mM TEAB. Proteins were digested with Lys-C for  
169 3 hours at 37 °C, followed by trypsin incubation for 16 hours at 37 °C. Enzymes were  
170 prepared with 50 mM TEAB, and 50 ng and 0.5 ng of enzymes were used to digest  
171 for 100 cells and a single cell, respectively (1  $\mu$ L solution was used). The plates were  
172 sealed with an adhesive plate seal for every incubation. After digestion, 4  $\mu$ L (40  $\mu$ g)  
173 TMT reagent in 0.5% acetic acid and 50% acetonitrile were added, and samples were

174 incubated for 60 min at 25 °C. The pH of the sample solutions during TMT labeling  
175 was approximately pH 8. To quench the TMT reaction, 1  $\mu$ L 30% hydroxylamine was  
176 added to each sample and incubated for 15 min at 25 °C. Subsequently, the  
177 surfactants were removed using the phase transfer method <sup>16,17</sup>. Briefly, sample  
178 solutions, including ethyl acetate, were combined and acidified with TFA to give a  
179 final concentration of 0.5%. The combined samples were mixed by vortexing and then  
180 centrifuged at 15600  $\times g$  for 2 min. Ethyl acetate, including surfactants, was  
181 discarded. The peptides were purified using SDB-XC StageTip <sup>18,19</sup>.

182

### 183 **Sample preparation using the WinO method**

184 For the WinO digestion, 50  $\mu$ L ethyl acetate were added into the wells of a 96-well  
185 plate before adding 1  $\mu$ L extraction buffer (50 mM TEAB, 12 mM SDC, 12 mM SLS,  
186 and 0.125 units of benzonase). Cells were sorted into each well and spun at 300  $\times g$   
187 for 1 min at 25 °C to mix the extraction buffer droplets and cell droplets. After 30  
188 min incubation at RT, 1  $\mu$ L (3.3  $\mu$ g) carboxyl-coated Magnosphere beads equilibrated  
189 with 50 mM TEAB were added to each well. From the reduction step with 100 mM  
190 DTT, the sample preparation was performed as per the ISD method. The solutions  
191 were added into ethyl acetate.

192

### 193 **nanoLC-MS/MS analysis**

194 Three different mass-spectrometry systems were used in this study. To determine  
195 the optimum magnetic beads for the WinO method, a TripleTOF 5600 (Sciex,  
196 Framingham, MA) and an UltiMate 3000 RSLCnano (Thermo Fisher Scientific) were  
197 used. In this system, 5  $\mu$ L was injected into the LC system. The LC was performed  
198 using an Acclaim PepMap RSLC (75  $\mu$ m  $\times$  25 cm, C18, 2  $\mu$ m, Thermo Fisher  
199 Scientific) at 300 nL/min. The mobile phase consisted of (A) 0.1% formic acid and (B)  
200 0.1% formic acid in acetonitrile. Linear gradients of 2–25% B in 60 min, 50–90% B  
201 in 15 min, and 90% B for 5 min were applied, and the spray voltage was 2300 V. For  
202 information-dependent acquisition (IDA), the precursor scan range was *m/z* 300–  
203 1250 in 250 ms. The top 20 precursor ions with a charge of +2 to +5 were selected,  
204 and the product ion scan was performed for 50 ms over the range of *m/z* 100–1600.  
205 Sequential window acquisition of all theoretical fragment-ion spectra (SWATH) was  
206 performed with the LC method described for IDA using 73 variable windows with 40  
207 ms scan times. The product ions were collected in the range of *m/z* 100–1600 in high-  
208 sensitivity mode.

209 The 100-cell proteomic analysis utilizing the TMT reagents was performed on an  
210 Orbitrap Fusion Tribrid mass spectrometer (Thermo Scientific) and an EASY-nLC™  
211 1200 system (Thermo Scientific). Peptides were first loaded onto an Acclaim™  
212 PepMap™ 100 C18 (3  $\mu$ m, 75  $\mu$ m ID  $\times$  20 mm length, P/N 164946 Thermo Scientific),  
213 and then separated on C18 packed emitter column (3  $\mu$ m, 75  $\mu$ m I.D.  $\times$  150 mm  
214 length, Nikkyo Technos, Tokyo, Japan). The injection volume was 5  $\mu$ L and the flow  
215 rate was 300 nL/min. The mobile phase consisted of (A) 0.1% formic acid and (B)  
216 0.1% formic acid in 80% acetonitrile. A multiple-linear gradient elution was  
217 performed as follows: 5–35% B in 60 min, 35–100% B in 5 min, and 90% B for 10 min.  
218 Multiplex analysis using TMT reagents was performed using a synchronous  
219 precursor selection (SPS) MS3 scan in top-speed mode (cycle time = 3 sec). The  
220 parameters were as follows: spray voltage, 2300 V; temperature of the ion transfer  
221 tube, 250 °C; Orbitrap scan range for precursor ion ( $m/z$ ), 350–1500; resolution for  
222 precursor scan, 120,000; ion trap scan range ( $m/z$ ), auto; collision energy for MS2,  
223 35%, collision mode for MS2, CID; collision energy for MS3, 65%; collision mode for  
224 MS3, HCD; Orbitrap scan range for MS3 ( $m/z$ ), 100–500; resolution for reporter ion  
225 detection, 50,000; maximum injection time, 50 ms for MS1 and MS2 scan, 105 ms for  
226 MS3 scan; AGC target, 400,000 for MS1 orbitrap, 10,000 for MS2 ion trap, 100,000  
227 for MS3 orbitrap.

228 For single-cell proteomics utilizing the TMT reagents, we performed the SPS MS3  
229 scan with a real-time search based on an Orbitrap Eclipse Tribrid mass spectrometer  
230 (Thermo Scientific) with FAIMS Pro interface (Thermo Scientific) and an EASY-  
231 nLC™ 1200 system (Thermo Scientific) equipped with an Aurora column (75  $\mu$ m I.D.,  
232 15 cm length, 1.6  $\mu$ m beads, IonOpticks, Fitzroy, Australia). The mobile phase  
233 consisted of (A) 0.1% formic acid and (B) 0.1% formic acid in 80% acetonitrile. LC  
234 gradients of 6–20% B in 37 min, 20–30% B in 14 min, 30–40% B in 9 min, 30–90% B  
235 in 3 min, and 90% B for 7 min were applied. For the SPS MS3 scan, the parameters  
236 were as follows: flow rate, 300 nL/min; spray voltage, 2000 V; temperature of ion  
237 transfer tube, 275 °C; Orbitrap scan range for precursor ion ( $m/z$ ), 375–1500;  
238 resolution for precursor scan, 60,000; FAIMS CV, -50 and -70; ion trap scan range  
239 ( $m/z$ ), 200–1200; collision energy for MS2, 30%; collision mode for MS2, CID;  
240 injection time for MS2 (ms), 500; collision energy for MS3, 65%; collision mode for  
241 MS3, HCD; Orbitrap scan range for MS3 ( $m/z$ ), 100–500; reporter ion detection  
242 resolution, 50,000; injection time for MS3 (ms), 500; AGC target, 200% (1E5). The  
243 parameters for the real-time search were as follows: enzyme, trypsin; maximum

244 search time (ms), 100; SPS mode, true; Xcorr, 1.4; sCn, 0.1; precursor, 10 ppm;  
245 precursor range (*m/z*), 400–1200; precursor exclusion, low 25 ppm and high 25 ppm.

246

247 **Data analysis**

248 The IDA and SWATH data obtained by the TripleTOF 5600 were analyzed using  
249 ProteinPilot version 4.5 (Sciex) and PeakView version 2.1 (Sciex). The false discovery  
250 rate (FDR) was estimated by searching against a decoy database generated by  
251 randomization of the UniProt human reference database. The data obtained from  
252 the Orbitrap Fusion Tribrid mass spectrometer was analyzed using MaxQuant <sup>20</sup>  
253 ver.1.6.17.0, and the UniProt human reference database was used as the reference.  
254 The parameters were as follows: type of parameter section, reporter ion MS3;  
255 isobaric labels, 10plex TMT or 11plex TMT; enzyme, trypsin/P; variable  
256 modifications, oxidation (M) and acetyl (protein N-term); and fixed modifications,  
257 carbamidomethyl (C). For the data obtained from the Orbitrap Eclipse Tribrid mass  
258 spectrometer, we used Proteome Discoverer ver.2.5 (Thermo). The parameters were  
259 as follows: enzyme, trypsin (full); maximum missed cleavage site, 2; and dynamic  
260 modification, oxidation (M), acetyl (N-terminal of protein), Met-loss (N-terminal of  
261 protein), and Met-loss+ acetyl (N-terminal of protein); static modification,  
262 carbamidomethyl (C); minimum average reporter S/N, 10. According to a previous  
263 report, the grand average of hydropathy (GRAVY) scores of proteins and peptides  
264 were calculated <sup>21</sup>. For gene ontology (GO) analysis, we used DAVID version 6.7  
265 (<https://david.ncifcrf.gov/summary.jsp>). Uniform manifold approximation and  
266 projection (UMAP) was generated using the R script. The *t* test was performed using  
267 GraphPad Prism 8.4.3 (GraphPad Software, CA) or Excel (Microsoft, MA). One-way  
268 ANOVA Tukey's multiple comparison test was performed using GraphPad Prism  
269 8.4.3. Statistical significance in the proteomics data was considered for fold changes  
270  $\geq 2$  or  $\leq 0.5$  with a *p*-value  $< 0.05$ .

271

272

273

274

275 **Results and discussion**

276 **1. Effect of the WinO method on the recovery of small samples**

277 In the WinO method, a 1- $\mu$ L water droplet containing 50 mM TEAB, 12 mM SDC,  
278 12 mM SLS, and 0.125 units benzonase was formed in 50  $\mu$ L ethyl acetate (Figure  
279 1A). The SDC and SLS have been reported to enhance protein extraction and  
280 digestion efficiencies of Lys-C and trypsin<sup>16,17</sup>. In addition, SDC and SLS are known  
281 as phase transfer surfactants (PTSs), which can be removed from peptide solutions  
282 by a phase transfer method<sup>16,17</sup>. To enhance the protein extraction from cells, heating,  
283 ultrasonication, and freezing/thawing are generally used. In the WinO method, these  
284 treatments are not possible because ethyl acetate is volatile, or sample solution and  
285 ethyl acetate are mixed during these treatments. Hence, we assessed differences in  
286 extraction efficiency between ultrasonication and heating in the PTS solution and a  
287 solution prepared by mixing cells in the PTS solution (Figure S1). The protein  
288 amount, number, and intensity of quantified proteins and peptides were comparable  
289 between the two methods. Therefore, ultrasonication and heat treatment were not  
290 used for the protein extraction process in this study. The magnetic beads, DTT, IAA,  
291 Lys-C, and trypsin solutions prepared in 50 mM TEAB were added to ethyl acetate.  
292 These solutions form water droplets in ethyl acetate, which merge with the sample  
293 droplet. The digested peptides were labeled by adding the TMT solution; after  
294 combining multiple samples, SDC and SLS were removed using the phase transfer  
295 method<sup>16,17</sup> (Figure 1B). The peptides purified with StageTip were analyzed by  
296 nanoLC-MS/MS.

297 To examine whether the proteins and peptides were retained in the water droplet  
298 in ethyl acetate, 10  $\mu$ g HEK293 whole cell lysate or 10  $\mu$ g digested peptides solution  
299 were added into ethyl acetate and incubated for 24 h. Ethyl acetate and water  
300 droplets were collected, and the distribution of each fraction was confirmed by SDS-  
301 PAGE and nanoLC-MS/MS for proteins and peptides, respectively. As controls,  
302 whole-cell lysates or peptide solutions were also used for SDS-PAGE or nanoLC-  
303 MS/MS along with the treated samples. In addition, unloaded samples without  
304 proteins or peptides were prepared as negative control samples. To examine protein  
305 retention in water droplets in ethyl acetate using SDS-PAGE, smears of proteins  
306 larger than 100 kDa and smaller than 25 kDa were detected in the ethyl acetate  
307 fraction (Figure S2A). These smears were also detected in the ethyl acetate fraction  
308 of the unloaded negative control samples. No other protein bands were detected in  
309 the ethyl acetate fraction of the protein-loaded group (Figure S2A). Next, we  
310 examined the distribution of the peptides in ethyl acetate and the sample droplet.

311 There was no significant difference in the total peak area of the peptides detected in  
312 the control and sample droplet fractions ( $p = 0.5734$ , Figure S2B). The percent  
313 composition of the peptide peak area quantified in the ethyl acetate fraction was only  
314 0.12%. The total peak area of peptides in this fraction showed no significant  
315 difference from that in the ethyl acetate fraction of negative control ( $p = 0.0561$ )  
316 (Figure S2B). These results suggest that proteins and peptides are retained in water  
317 droplets for at least 24 hours.

318 Next, we performed the WinO method using sorted cells as starting material,  
319 which was then compared to the recovery of peptides (Table S1) and proteins (Table  
320 S2) in the ISD method. The WinO method was performed as described above. In the  
321 ISD method, surfactant solution was added into the well of a 96-well plate before 100  
322 cells were injected into the solution using a cell sorter. Next, the DTT, IAA, Lys-C,  
323 and trypsin solutions were added directly into the sample solution. TMT-labeled  
324 peptides corresponding to 5000 cells as carriers were combined with the 100-cell  
325 samples from the ISD and WinO methods. The carrier was used to increase peptide  
326 and protein identification, as well as reduce peptide loss after digestion as SCoPE-  
327 MS <sup>11</sup>. The peptide intensity in the WinO method was significantly higher than that  
328 in the ISD method ( $p < 0.0001$ ;  $n = 3$ , Figure 2A). Next, we compared the recovery of  
329 the peptides quantified in all data. The intensity of 1018 out of 1177 peptides (86.5%)  
330 increased significantly ( $\geq 2$ -fold,  $p < 0.05$ ) in the WinO method, whereas the intensity  
331 of none of the peptides increased significantly in the ISD method (Figure 2B). The  
332 median relative peptide recovery from WinO was 6.70-fold greater than that from  
333 the ISD method. The number of quantified peptides increased only 1.3-fold ( $p =$   
334 0.0199) when the WinO method ( $2071.7 \pm 34.4$ ) was used compared to the ISD  
335 method ( $1598.3 \pm 215.9$ ). In this study, we counted the proteins in which reporter ions  
336 were detected. The triggering of MS2 was assisted by the carrier, which reduced the  
337 difference in the number of detected proteins between the two methods. To examine  
338 the reproducibility of the WinO method, we compared the % coefficient of variations  
339 (CVs) of peptide levels in triplicate between the two methods. The %CV distribution  
340 pattern using the WinO method was lower than that with the ISD method (Figure  
341 2C), with median %CVs of 39.6% and 14.4% for ISD and WinO methods, respectively.

342 Next, we evaluated the digestion efficiency of the WinO method by measuring the  
343 levels of mis-cleaved peptides. Lys-C and trypsin solutions were delivered to the  
344 sample droplets through ethyl acetate in the WinO method, and 8.03 g ethyl acetate  
345 was dissolved in 100 mL water at room temperature <sup>22</sup>. It was expected that the  
346 dissolved ethyl acetate affects the activity of Lys-C and trypsin. However, mis-

347 cleavage of the total peptides in the WinO method ( $9.9 \pm 0.4\%$ ) was significantly  
348 lower than that in the ISD method ( $17.1 \pm 2.2\%$ ) (Figure 2D). In addition, the  
349 improvement in peptide recovery from fully cleaved peptides was significantly higher  
350 ( $p < 0.0001$ ) than in the mis-cleaved peptides using the WinO method (Figure S3).  
351 Contrary to expectations, the digestion efficiency of the WinO method was enhanced  
352 compared to that of the ISD method. It was reported that the activities of proteolytic  
353 enzymes are enhanced in the presence of organic solvents, such as methanol,  
354 isopropyl alcohol, and acetonitrile <sup>23</sup>. It is likely that the dissolved ethyl acetate in  
355 the sample droplet enhanced Lys-C and trypsin activities in the WinO method.  
356 Moreover, the reduction in the adsorption loss of Lys-C and trypsin maintained a  
357 high enzyme concentration in the sample droplet. Although the recovery of proteins  
358 was overall improved with the WinO method, a significant negative correlation ( $r =$   
359  $-0.1794$ ,  $p < 0.0001$ ) was observed in protein hydrophobicity, as evidenced by the  
360 GRAVY score and protein recovery (Figure 2E). A greater score indicates a more  
361 hydrophobic protein/peptide in GRAVY score. This indicated that the WinO method  
362 led to a higher recovery of hydrophilic than hydrophobic proteins.

363 Based on these results, we speculated that the 100-cell protein and peptide  
364 recoveries were enhanced with the WinO method due to the reduced contact surface  
365 area between the sample solution and plastic tubes, as well as the improved  
366 digestion efficiency of trypsin and Lys-C. However, the improvement in hydrophobic  
367 protein recovery was lower than that in hydrophilic proteins, possibly due to lower  
368 retention of these proteins in the ethyl acetate solution than hydrophilic proteins.  
369

## 370 **2. Effect of carboxyl-coated magnetic beads on peptides recovery using the WinO 371 method**

372 To enhance the recovery of hydrophobic proteins and peptides, we tried to retain  
373 them in the sample droplet using beads. To select beads with high peptide recovery  
374 for the WinO method, we examined six different types of beads, an amine-, a methyl  
375 sulfonate-, a sulfopropyl-, and three carboxyl-coated beads. The carboxyl-coated  
376 beads tended to show a higher total intensity of proteins than other bead types. The  
377 carboxyl-coated Magnosphere beads showed the highest recovery among all beads  
378 tested (Figure S4). Single-pot, solid-phase-enhanced sample preparation (SP3) <sup>24</sup> and  
379 protein aggregation capture (PAC) <sup>25</sup> have been reported as methods to retain  
380 peptides on beads. In SP3 and PAC, peptides are captured on the beads in organic  
381 solvent based on the hydrophilic interaction. In this study, proteins and peptides  
382 were retained on the beads in aqueous solution. Hence, we assumed that proteins

383 and peptides are retained on the beads via ionic interactions rather than hydrophilic  
384 interactions. In addition, it is likely that the hydrophobic parts of proteins and  
385 peptides have a high affinity with the beads because of the hydrophobic material of  
386 Magnosphere beads. We performed proteomic analysis of the 100 sorted cells using  
387 the WinO method with or without beads in triplicate (Tables S3 and S4 for peptides  
388 and proteins, respectively). After digestion, each sample was labeled with TMT  
389 reagent and mixed. The peptide level significantly increased in WinO samples  
390 combined with beads compared to WinO samples without beads ( $p < 0.0001$ ; Figure  
391 3A). Figure 3B shows the distribution of relative peptide levels ( $n = 1898$ ) in the  
392 WinO samples processed with beads compared to those without. The median peptide  
393 ratio was 1.497 (Figure 3B). The peptide ratio of 1825 out of 1898 peptides (96.2%)  
394 was higher in samples prepared with the beads than without beads. Moreover, there  
395 was no significant difference in the percentage of cleaved peptides (Figure 3C),  
396 suggesting that the addition of beads does not affect the Lys-C and trypsin activities.  
397 The reproducibility of the WinO method was evaluated by comparing the protein  
398 levels from triplicate analyses (Figure 3D). The Pearson correlations for all pairs  
399 were higher than 0.96, indicating that the reproducibility of peptide quantification  
400 was unaffected by the presence of beads. Thus, we combined the beads with the WinO  
401 method in subsequent experiments.

402 We characterized proteins and peptides whose recovery was improved by the  
403 addition of beads. Figure 4A shows the correlation of protein recovery and GRAVY  
404 score. The hydrophobicity of proteins did not correlate with their recovery; in other  
405 words, the protein recovery rate improved independently of their hydrophobicity.  
406 Next, the Spearman correlation coefficient was calculated by comparing the recovery  
407 rate of peptides with the frequency of each amino acid and GRAVY score (Figure 4B).  
408 A significant positive correlation was observed in the GRAVY score and the peptide  
409 recovery ( $r = 0.0810$ ,  $p = 0.0004$ ; Figure 4B). In addition, the frequency of the basic  
410 amino acids (H, K, and R) showed the highest coefficient ( $r = 0.1067$ ,  $p < 0.0001$ ,  
411 Figure 4B, Figure S5), whereas the frequency of acidic amino acids (D and E) showed  
412 the lowest coefficient ( $r = -0.1162$ ,  $p < 0.0001$ ; Figure 4B, Figure S5). The recovery of  
413 basic and hydrophobic peptides, which had a high affinity for beads in the basic  
414 condition, was improved by the WinO method. Although acidic amino acid showed a  
415 negative correlation coefficient with peptide recovery, the peptide and protein  
416 recoveries improved overall in the WinO samples combined with beads (Figure 3A,  
417 3B, and Figure 4A).

418

419 **3. Comparison of the proteome profiles obtained with the ISD and WinO methods**

420 To date, none of the proteomic approaches have evaluated water droplets formed in the  
421 oil. Therefore, it was unclear whether the proteome profiles obtained by the WinO  
422 method were comparable to those obtained using the conventional ISD method. To  
423 examine the similarity of the proteome profiles between these two methods, we  
424 compared the proteome profile of 100 cells processed with the WinO method with  
425 that of 10000 cells processed with the ISD method using 15 multiple myeloma cell  
426 lines (Figure 5). The cells were sorted into a 96-well plate for the WinO method and  
427 into 1.5 mL tubes for the ISD method. From the 100-cell group, an average of 2183.6  
428  $\pm$  74.5 peptides were quantified (Table S5), whereas an average of 29293.0  $\pm$  561.2  
429 peptides were quantified from the 10000-cell group (Figure 6A, Table S6). From these  
430 peptides, an average of  $592.9 \pm 13.2$  proteins were quantified from the 100-cell group  
431 (Table S7), whereas an average of  $4651.6 \pm 91.6$  proteins were quantified from the  
432 10000-cell group (Figure 6B, Table S8). In total, 798 proteins were quantified from  
433 the 15 strains using the WinO method, among which 387 proteins were found in all  
434 cell lines. Using the ISD method with 10000 cells, 5545 proteins were identified, with  
435 3584 proteins found in all cell lines. Next, we compared the expression profiles of the  
436 377 proteins that were quantified in both methods. Normalized expression levels  
437 were plotted using the UMAP algorithm (Figure 6C). The proteome profiles of 100  
438 and 10000 cells were plotted close to each other and formed populations among the  
439 same cell line, even though the sample preparation method and the number of cells  
440 were different. The median %CV of the protein level for the 100-cell group (14.1%, n  
441 = 5805) was higher than that for the 10000-cell group (3.0%, n = 53760; Figure S6).  
442 The reduced reproducibility in the 100-cell group could be due to cellular heterogeneity  
443 in a limited sample, as well as higher variability in sample preparation from a small  
444 number of cells.

445 Gene-ontology (GO) analysis of 798 proteins identified ribosomal proteins,  
446 proteasome-related proteins, and enzymes of the central carbon metabolism system  
447 (Figure 7A). In addition to these abundant proteins, transmembrane proteins  
448 (TMPs) and cell adhesion-related proteins were identified. To examine the effect of  
449 the WinO method on the recovery of TMPs, we compared the distribution of the  
450 number of transmembrane domains (TMDs) between 832 TMPs identified with the  
451 ISD method using 10000 cells with the 70 TMPs identified by the WinO method  
452 using 100 cells (Figure 7B). We found that the distribution patterns were highly  
453 correlated ( $r = 0.9826$ ,  $p < 0.0001$ ). TMPs are some of the most difficult proteins to  
454 identify using proteomics, and proteins with more TMDs are generally more difficult

455 to extract and identify<sup>26,27</sup>. The WinO method uses the PTS as protein extraction  
456 developed for membrane proteomics<sup>16,17</sup>. These results indicated that the PTS  
457 improved the extraction and digestion efficiencies of membrane proteins, as well as  
458 soluble proteins. Thus, these results provided evidence that the WinO method-based  
459 proteomic analysis combined with PTS was an effective and unbiased approach for  
460 100-cell proteomics.

461

#### 462 **4. Single-cell proteomic analysis using the WinO method**

463 Finally, we examined the applicability of the WinO method for single-cell proteomics.  
464 Single RPMI8226 cells were directly sorted into a 96-well plate, and proteins were  
465 digested using the ISD or WinO method in quadruplicate. Peptides were labeled with  
466 TMT reagents and combined with TMT-labeled peptides that corresponded to 50 cells.  
467 The combined samples were then analyzed by nanoLC-MS/MS using an Orbitrap  
468 Eclipse, identifying 845 proteins and 2493 peptides. Of these identified proteins and  
469 peptides, 462 proteins (Table S9) and 1506 peptides (Table S10) were quantified. The  
470 average number of quantified peptides was  $227.0 \pm 114.5$  and  $1177.8 \pm 131.6$  for the  
471 ISD and WinO method, respectively (Figure 8A). The average number of quantified  
472 proteins was  $140.8 \pm 51.8$  and  $400.3 \pm 32.5$  for the ISD and WinO method,  
473 respectively (Figure 8A). The numbers of these peptides and proteins were  
474 significantly higher in the WinO method at 5.2-fold ( $p < 0.0001$ ) and 2.8-fold ( $p <$   
475  $0.0001$ ), respectively (Figure 8A). Furthermore, to examine the effect of the WinO  
476 method on protein recovery, we compared the levels of proteins quantified by both  
477 methods. Figure 8B shows a volcano plot that compares 247 commonly identified  
478 proteins in both methods, indicating that the contents of 221 out of 247 proteins  
479 significantly ( $p < 0.05$ ) increased 2-fold or more with the WinO method. There were  
480 no proteins significantly decreased in the WinO method. The median relative  
481 recovery of proteins was 10.21-fold greater with the WinO method than the ISD  
482 method. The levels of proteins commonly identified using both methods were  
483 significantly higher ( $p < 0.0001$ ) than those uniquely identified using the WinO  
484 method (Figure 8C). These results suggested that the number of quantified proteins  
485 and peptides increased by increasing their recovery by the WinO method using single  
486 cells. In addition, 33 TMPs including one cluster of differentiation (CD) protein,  
487 CD71, were quantified in this study; among them, 24 TMPs were uniquely quantified  
488 using the WinO method. RapiGest<sup>13</sup> and n-dodecyl- $\beta$ -D-maltoside<sup>14</sup> have been used  
489 for protein extraction in single-cell proteomics. It has been reported that these  
490 additives have comparable or higher solubility of membrane proteins than SDC<sup>17</sup>,

491 which was used in the WinO method. However, the Lys-C and trypsin activities were  
492 higher in the presence of SDC than these additives, resulting in a higher number of  
493 hydrophobic proteins and peptides identified <sup>17</sup>. In this study, we used a mixture of  
494 SDC and SLS, which is known to considerably increase the solubility and the number  
495 of membrane as well as soluble proteins compared with SDC alone <sup>16</sup>. These findings  
496 suggest that the extraction efficiency of proteins from a single cell is higher in the  
497 WinO method than in other single-cell proteomic techniques. Our WinO method  
498 enhanced protein recovery and protein identification not only soluble proteins but  
499 also TMPs from single cells, thereby highlighting its application for the single-cell  
500 proteomic analysis.

501

## 502 **Conclusions**

503 On the WinO method, cells were directly injected into the sample droplet by a cell  
504 sorter. The method does not require any specialized equipment. The recovery of  
505 proteins and peptides is dramatically increased compared to the ISD method by  
506 reducing the contact area between the sample solution and the plastic container. In  
507 addition, the pipette tip does not contact the sample solution when the DTT, IAA,  
508 Lys-C, trypsin, and TMT solutions are added; thus, protein loss due to adsorption  
509 onto the pipette tip is avoided. Although there are still limitations to this method,  
510 such as the possibility of a lower peptide recovery rate once ethyl acetate is removed,  
511 the recovery of peptides and proteins increased approximately 10-fold for single-cell  
512 proteomics by coupling the use of phase transfer surfactants and carboxyl-coated  
513 hydrophobic beads. Several methods for single-cell proteomics have been previously  
514 reported <sup>11,14,28</sup>. It is hardly possible to directly compare these methods in terms of  
515 numbers of quantified proteins due to differences in analytic systems and equipment.  
516 Nevertheless, we conclude that when compared to the ISD method, our novel  
517 strategy further improves the sensitivity of single-cell proteomics. In addition,  
518 although the WinO method was successfully performed on 96-well plates, we expect  
519 that the method is scalable to 384- and 1536-well plates using liquid handling robots,  
520 further enhancing the throughput of single-cell proteomics.

521

## 522 **Associated content**

### 523 **Supporting Information**

- 524 1. Supporting figures (PDF)
- 525 2. Table S1: Peptides identified from 100 cells by the ISD and WinO methods  
526 (XLSX)

527 3. Table S2: Proteins identified from 100 cells by the ISD and WinO methods (XLSX)  
528 4. Table S3: Peptides identified from 100 cells using the WinO method with or  
529 without beads (XLSX)  
530 5. Table S4: Proteins identified from 100 cells using the WinO method with or  
531 without beads (XLSX)  
532 6. Table S5: Peptides identified from 100 cells by the WinO method (XLSX)  
533 7. Table S6: Proteins identified from 10000 cells by the ISD method (XLSX)  
534 8. Table S7: Proteins identified from 100 cells by the WinO method (XLSX)  
535 9. Table S8: Proteins identified from 10000 cells by the ISD method (XLSX)  
536 10. Table S9: Proteins identified from single cell by the ISD and WinO methods  
537 (XLSX)  
538 11. Table S10: Peptides identified from single cell by the ISD and WinO methods  
539 (XLSX)  
540 12. The MS raw data and result files have been deposited in the ProteomeXchange  
541 Consortium (<http://www.proteomexchange.org/>, PXD029814) via the jPOST  
542 partner repository (<https://jpostdb.org>, JPST001390) <sup>29</sup>.

543

## 544 **Author Information**

### 545 **Corresponding Author**

546 **Takeshi Masuda** - *Department of Pharmaceutical Microbiology, Faculty of Life*  
547 *Sciences, Kumamoto University, Chuo-ku, Kumamoto, 862-0973, Japan;*  
548 <http://orcid.org/0000-0003-0121-4783>; Email: [tmasuda@kumamoto-u.ac.jp](mailto:tmasuda@kumamoto-u.ac.jp)

549

### 550 **Authors**

551 **Yuma Inamori** - *Department of Pharmaceutical Microbiology, Graduate School of*  
552 *Pharmaceutical Sciences, Kumamoto University, Chuo-ku, Kumamoto, 862-0973,*  
553 *Japan*

554 **Arisu Furukawa** - *Department of Pharmaceutical Microbiology, Graduate School of*  
555 *Pharmaceutical Sciences, Kumamoto University, Chuo-ku, Kumamoto, 862-0973,*  
556 *Japan*

557 **Kazuki Momosaki** - *Department of Pharmaceutical Microbiology, Graduate School of*  
558 *Pharmaceutical Sciences, Kumamoto University, Chuo-ku, Kumamoto, 862-0973,*  
559 *Japan*

560 **Chih-Hsiang Chang** - *Department of Tumor Genetics and Biology, Graduate School*  
561 *of Medical Sciences, Kumamoto University, Chuo-ku, Kumamoto, 860-8556, Japan;*  
562 <https://orcid.org/0000-0002-0029-5385>

563 **Daiki Kobayashi** - *Department of Tumor Genetics and Biology, Graduate School of*  
564 *Medical Sciences, Kumamoto University, Chuo-ku, Kumamoto, 860-0811, Japan*  
565 *Department of Omics Biology, Graduate School of Medical and Dental Sciences,*  
566 *Niigata University, Niigata, 951-8510, Japan;* <https://orcid.org/0000-0003-4131-5220>  
567 **Hiroto Ohguchi** - *Division of Disease Epigenetics, Institute of Resource Development*  
568 *and Analysis, Kumamoto University, Chuo-ku, Kumamoto, 860-0811, Japan*  
569 **Yawara Kawano** - *Department of Hematology, Rheumatology, and Infectious*  
570 *Diseases, Faculty of Life Sciences, Kumamoto University, Kumamoto, 860-0811,*  
571 *Japan;* <https://orcid.org/0000-0002-8269-440X>  
572 **Shingo Ito** - *Department of Pharmaceutical Microbiology, Faculty of Life Sciences,*  
573 *Kumamoto University, Chuo-ku, Kumamoto, 862-0973, Japan*  
574 **Norie Araki** - *Department of Tumor Genetics and Biology, Graduate School of*  
575 *Medical Sciences, Kumamoto University, Chuo-ku, Kumamoto, 860-8556, Japan;*  
576 <https://orcid.org/0000-0001-9987-6229>  
577 **Shao-En Ong** - *University of Washington, Department of Pharmacology, Seattle, WA*  
578 *98195, United States;* <https://orcid.org/0000-0003-3314-5903>  
579 **Sumio Ohtsuki** - *Department of Pharmaceutical Microbiology, Faculty of Life*  
580 *Sciences, Kumamoto University, Chuo-ku, Kumamoto, 862-0973, Japan;*  
581 <http://orcid.org/0000-0003-4634-7133>  
582

## 583 **Author Contributions**

584 Conceptualization, T.M.; Investigation, T.M., Y.I., A.F., K.M., C.H.C., and D.K.;  
585 Formal analysis; T.M.; Resources, T.M., H.O., Y.K., and M.M.; Writing-original draft,  
586 T.M.; Funding acquisition, T.M., S.E.O., and S.O.; Supervision, writing-review and  
587 editing, T.M., S.I., N.A., S.E.O., and S.O.

588

## 589 **Notes**

590 The Authors declare no competing financial interest.

591

## 592 **Acknowledgments**

593 We thank Shio Watanabe, Kentaro Takahara, and Daisuke Higo from Thermo Fisher  
594 Scientific for conducting the single-cell proteomic analysis. This work was supported  
595 by JSPS KAKENHI Grant Numbers JP17K15042 and JP 19K05544 to T.M. This  
596 work was also supported by the Adaptable and Seamless Technology Transfer  
597 Program through Target-driven R&D (A-STEP) Grant Number JPMJTR20UM, and  
598 a Fusion Oriented Research for Disruptive Science and Technology Grant from

599 Japan Science and Technology Agency (JST), and COCKPI-T Funding from Takeda  
600 Pharmaceutical Company Limited to T.M. This work was supported by JST-CREST  
601 (Grant Number JP171024167) to S.O. This work was also supported by grants from  
602 the National Institutes of Health issued under the award numbers R01AR065459  
603 and R01GM129090 (S-E.O.)  
604

## 605 References

606

607 (1) Patel, A. P.; Tirosh, I.; Trombetta, J. J.; Shalek, A. K.; Gillespie, S. M.; Wakimoto, H.; Cahill, D. P.; Nahed, B. V.; Curry, W. T.; Martuza, R. L.; Louis, D. N.; Rozenblatt-  
608 Rosen, O.; Suva, M. L.; Regev, A.; Bernstein, B. E. Single-Cell RNA-Seq Highlights  
609 Intratumoral Heterogeneity in Primary Glioblastoma, *Science* **2014**, *344*, 1396-1401.

610 (2) Jerby-Arnon, L.; Shah, P.; Cuoco, M. S.; Rodman, C.; Su, M. J.; Melms, J. C.;  
611 Leeson, R.; Kanodia, A.; Mei, S.; Lin, J. R.; Wang, S.; Rabasha, B.; Liu, D.; Zhang,  
612 G.; Margolais, C.; Ashenbergs, O.; Ott, P. A.; Buchbinder, E. I.; Haq, R.; Hodi, F. S., et  
613 al. A Cancer Cell Program Promotes T Cell Exclusion and Resistance to Checkpoint  
614 Blockade, *Cell* **2018**, *175*, 984-997 e924.

615 (3) Levitin, H. M.; Yuan, J.; Sims, P. A. Single-Cell Transcriptomic Analysis of Tumor  
616 Heterogeneity, *Trends Cancer* **2018**, *4*, 264-268.

617 (4) Achim, K.; Pettit, J. B.; Saraiva, L. R.; Gavriouchkina, D.; Larsson, T.; Arendt,  
618 D.; Marioni, J. C. High-Throughput Spatial Mapping of Single-Cell RNA-Seq Data to  
619 Tissue of Origin, *Nat. Biotechnol.* **2015**, *33*, 503-509.

620 (5) Jaitin, D. A.; Kenigsberg, E.; Keren-Shaul, H.; Elefant, N.; Paul, F.; Zaretsky, I.;  
621 Mildner, A.; Cohen, N.; Jung, S.; Tanay, A.; Amit, I. Massively Parallel Single-Cell  
622 RNA-Seq for Marker-Free Decomposition of Tissues into Cell Types, *Science* **2014**,  
623 *343*, 776-779.

624 (6) Chen, H.; Albergante, L.; Hsu, J. Y.; Lareau, C. A.; Lo Bosco, G.; Guan, J.; Zhou,  
625 S.; Gorban, A. N.; Bauer, D. E.; Aryee, M. J.; Langenau, D. M.; Zinovyev, A.;  
626 Buenrostro, J. D.; Yuan, G. C.; Pinello, L. Single-Cell Trajectories Reconstruction,  
627 Exploration and Mapping of Omics Data with Stream, *Nat. Commun.* **2019**, *10*, 1903.

628 (7) Nam, A. S.; Kim, K. T.; Chaligne, R.; Izzo, F.; Ang, C.; Taylor, J.; Myers, R. M.;  
629 Abu-Zeinah, G.; Brand, R.; Omans, N. D.; Alonso, A.; Sheridan, C.; Mariani, M.; Dai,  
630 X.; Harrington, E.; Pastore, A.; Cubillos-Ruiz, J. R.; Tam, W.; Hoffman, R.; Rabadan,  
631 R., et al. Somatic Mutations and Cell Identity Linked by Genotyping of  
632 Transcriptomes, *Nature* **2019**, *571*, 355-360.

633 (8) Psaila, B.; Wang, G.; Rodriguez-Meira, A.; Li, R.; Heuston, E. F.; Murphy, L.; Yee,  
634 D.; Hitchcock, I. S.; Sousos, N.; O'Sullivan, J.; Anderson, S.; Senis, Y. A.; Weinberg,  
635 O. K.; Calicchio, M. L.; Center, N. I. H. I. S.; Iskander, D.; Royston, D.; Milojkovic,  
636 D.; Roberts, I.; Bodine, D. M., et al. Single-Cell Analyses Reveal Megakaryocyte-  
637 Biased Hematopoiesis in Myelofibrosis and Identify Mutant Clone-Specific Targets,  
638 *Mol. Cell* **2020**, *78*, 477-492 e478.

639 (9) Fortelny, N.; Overall, C. M.; Pavlidis, P.; Freue, G. V. C. Can We Predict Protein

640

641 from Mrna Levels?, *Nature* **2017**, *547*, E19-E20.

642 (10) Liu, Y.; Beyer, A.; Aebersold, R. On the Dependency of Cellular Protein Levels  
643 on Mrna Abundance, *Cell* **2016**, *165*, 535-550.

644 (11) Budnik, B.; Levy, E.; Harmange, G.; Slavov, N. Scope·Ms: Mass Spectrometry of  
645 Single Mammalian Cells Quantifies Proteome Heterogeneity During Cell  
646 Differentiation, *Genome Biol.* **2018**, *19*, 161.

647 (12) Williams, S. M.; Liyu, A. V.; Tsai, C. F.; Moore, R. J.; Orton, D. J.; Chrisler, W.  
648 B.; Gaffrey, M. J.; Liu, T.; Smith, R. D.; Kelly, R. T.; Pasa-Tolic, L.; Zhu, Y. Automated  
649 Coupling of Nanodroplet Sample Preparation with Liquid Chromatography-Mass  
650 Spectrometry for High-Throughput Single-Cell Proteomics, *Anal. Chem.* **2020**, *92*,  
651 10588-10596.

652 (13) Zhu, Y.; Piehowski, P. D.; Zhao, R.; Chen, J.; Shen, Y.; Moore, R. J.; Shukla, A.  
653 K.; Petyuk, V. A.; Campbell-Thompson, M.; Mathews, C. E.; Smith, R. D.; Qian, W.  
654 J.; Kelly, R. T. Nanodroplet Processing Platform for Deep and Quantitative Proteome  
655 Profiling of 10-100 Mammalian Cells, *Nat. Commun.* **2018**, *9*, 882.

656 (14) Tsai, C. F.; Zhang, P.; Scholten, D.; Martin, K.; Wang, Y. T.; Zhao, R.; Chrisler, W.  
657 B.; Patel, D. B.; Dou, M.; Jia, Y.; Reduzzi, C.; Liu, X.; Moore, R. J.; Burnum-Johnson,  
658 K. E.; Lin, M. H.; Hsu, C. C.; Jacobs, J. M.; Kagan, J.; Srivastava, S.; Rodland, K. D.,  
659 et al. Surfactant-Assisted One-Pot Sample Preparation for Label-Free Single-Cell  
660 Proteomics, *Commun. Biol.* **2021**, *4*, 265.

661 (15) Zhang, X. Less Is More: Membrane Protein Digestion Beyond Urea-Trypsin  
662 Solution for Next-Level Proteomics, *Mol. Cell. Proteomics* **2015**, *14*, 2441-2453.

663 (16) Masuda, T.; Saito, N.; Tomita, M.; Ishihama, Y. Unbiased Quantitation of  
664 Escherichia Coli Membrane Proteome Using Phase Transfer Surfactants, *Mol. Cell.*  
665 *Proteomics* **2009**, *8*, 2770-2777.

666 (17) Masuda, T.; Tomita, M.; Ishihama, Y. Phase Transfer Surfactant-Aided Trypsin  
667 Digestion for Membrane Proteome Analysis, *J. Proteome Res.* **2008**, *7*, 731-740.

668 (18) Rappaport, J.; Ishihama, Y.; Mann, M. Stop and Go Extraction Tips for Matrix-  
669 Assisted Laser Desorption/Ionization, Nanoelectrospray, and LC/MS Sample  
670 Pretreatment in Proteomics, *Anal. Chem.* **2003**, *75*, 663-670.

671 (19) Rappaport, J.; Mann, M.; Ishihama, Y. Protocol for Micro-Purification,  
672 Enrichment, Pre-Fractionation and Storage of Peptides for Proteomics Using  
673 Stagetips, *Nat. Protoc.* **2007**, *2*, 1896-1906.

674 (20) Cox, J.; Mann, M. Maxquant Enables High Peptide Identification Rates,  
675 Individualized P.P.B.-Range Mass Accuracies and Proteome-Wide Protein  
676 Quantification, *Nat. Biotechnol.* **2008**, *26*, 1367-1372.

677 (21) Kyte, J.; Doolittle, R. F. A Simple Method for Displaying the Hydropathic  
678 Character of a Protein, *J. Mol. Biol.* **1982**, *157*, 105-132.

679 (22) Altshuller, A. P.; Everson, H. E. The Solubility of Ethyl Acetate in Water, *Journal*  
680 *of the American Chemical Society* **1953**, *75*, 1727.

681 (23) Guo, C.; Steinberg, L. K.; Henderson, J. P.; Gross, M. L. Organic Solvents for  
682 Enhanced Proteolysis of Stable Proteins for Hydrogen-Deuterium Exchange Mass  
683 Spectrometry, *Anal. Chem.* **2020**, *92*, 11553-11557.

684 (24) Hughes, C. S.; Moggridge, S.; Muller, T.; Sorensen, P. H.; Morin, G. B.; Krijgsveld,  
685 J. Single-Pot, Solid-Phase-Enhanced Sample Preparation for Proteomics  
686 Experiments, *Nat. Protoc.* **2019**, *14*, 68-85.

687 (25) Batth, T. S.; Tollenaere, M. X.; Ruther, P.; Gonzalez-Franquesa, A.; Prabhakar,  
688 B. S.; Bekker-Jensen, S.; Deshmukh, A. S.; Olsen, J. V. Protein Aggregation Capture  
689 on Microparticles Enables Multipurpose Proteomics Sample Preparation, *Mol. Cell.*  
690 *Proteomics* **2019**, *18*, 1027-1035.

691 (26) Helbig, A. O.; Heck, A. J.; Slijper, M. Exploring the Membrane Proteome--  
692 Challenges and Analytical Strategies, *J. Proteomics* **2010**, *73*, 868-878.

693 (27) Griffin, N. M.; Schnitzer, J. E. Overcoming Key Technological Challenges in  
694 Using Mass Spectrometry for Mapping Cell Surfaces in Tissues, *Mol. Cell.*  
695 *Proteomics* **2011**, *10*, R110 000935.

696 (28) Schoof, E. M.; Furtwangler, B.; Uresin, N.; Rapin, N.; Savickas, S.; Gentil, C.;  
697 Lechman, E.; Keller, U. A. D.; Dick, J. E.; Porse, B. T. Quantitative Single-Cell  
698 Proteomics as a Tool to Characterize Cellular Hierarchies, *Nat. Commun.* **2021**, *12*,  
699 3341.

700 (29) Okuda, S.; Watanabe, Y.; Moriya, Y.; Kawano, S.; Yamamoto, T.; Matsumoto, M.;  
701 Takami, T.; Kobayashi, D.; Araki, N.; Yoshizawa, A. C.; Tabata, T.; Sugiyama, N.;  
702 Goto, S.; Ishihama, Y. Jpostrepo: An International Standard Data Repository for  
703 Proteomes, *Nucleic Acids Res.* **2017**, *45*, D1107-D1111.

704

705

706 **Figure legends**

707 **Figure 1. Water droplet-in-oil digestion (WinO) method.**

708 One microliter of water droplet containing 0.125 units of benzonase, 3.3  $\mu$ g magnetic  
709 beads, 12 mM sodium deoxycholate (SDC), 12 mM sodium lauroyl sarcosinate (SLS),  
710 and 100 mM TEAB (pH 8.5) formed in ethyl acetate (A). The workflow of the WinO  
711 method is presented in (B); the cells are loaded into water droplets in ethyl acetate  
712 using a cell sorter. The solutions for reduction, alkylation, and digestion are added  
713 to the ethyl acetate. The peptides are labeled with TMT reagents and then combined.  
714 The peptides are purified using the StageTip and injected into the nanoLC-MS/MS.  
715

716 **Figure 2. Comparison of the in-solution digestion (ISD) and WinO methods.**

717 As starting material, 100 RPMI8226 cells were sorted and digested in triplicate  
718 using ISD and WinO methods. The scatter plot shows the levels of 1015 peptides  
719 quantified using these digestion methods (A). Peptide levels are represented as the  
720 average of triplicate data. Each bar shows the median. Paired *t*-test was performed  
721 using GraphPad Prism 8.4.3. The relative peptide levels between the WinO and ISD  
722 methods are shown as a volcano plot (B). Red dots indicate peptides with a significant  
723 change ( $p < 0.05$ , 2-fold or more). The distribution of %CV from the ISD and WinO  
724 methods is presented in (C). The %CV for peptide intensities was calculated from  
725 triplicate data generated using each method. The proportion of mis-cleaved peptides  
726 in the ISD and WinO methods is shown in (D). These proportions were calculated  
727 based on peptide levels and averaged across triplicate samples. Error bars indicate  
728 standard deviation. Unpaired *t*-test was performed using GraphPad Prism 8.4.3. The  
729 correlation between the GRAVY protein score and relative protein levels from the  
730 WinO to the ISD method is shown in (E). The GRAVY score of proteins was calculated  
731 as previously reported<sup>21</sup>. In this correlation, 561 proteins commonly quantified by  
732 both methods are shown. The Pearson correlation and *p*-values were calculated using  
733 GraphPad Prism 8.4.3.

734

735 **Figure 3. Effect of carboxyl-coated magnetic beads on the WinO method efficiency.**

736 One hundred RPMI8226 cells were sorted and digested in triplicate. The WinO  
737 method was performed with and without magnetic beads. Peptide levels are  
738 presented as the average of triplicate data. The scatter plot shows the levels of 1898  
739 peptides quantified using both methods (A). Each bar shows the median. Paired *t*-  
740 test was performed using GraphPad Prism 8.4.3. The distribution of relative peptide  
741 levels between the WinO method with and without beads are shown in (B). The

742 proportion of mis-cleaved peptides in the WinO method with and without beads is  
743 shown in (C). These proportions were calculated based on peptide level and averaged  
744 across triplicate samples. Error bars indicate standard deviation. Unpaired *t*-test  
745 was performed using GraphPad Prism 8.4.3. Correlation of protein levels between  
746 replicates (D). Simple linear regressions were performed using GraphPad Prism  
747 8.4.3.

748

749 **Figure 4. Recovery rate and characteristics of peptides using carboxyl-coated**  
750 **magnetic beads with the WinO method.**

751 The GRAVY score of proteins was calculated as previously reported <sup>21</sup>. The Pearson  
752 correlation and *p*-values were calculated using GraphPad Prism 8.4.3 (A). The  
753 Spearman correlation coefficient was calculated by comparing the recovery rate of  
754 peptides with the WinO method with or without beads (B). The frequency of each  
755 amino acid and GRAVY score is presented for the corresponding peptides. The one-  
756 letter amino acid code is indicated on the X-axis. \*\* indicates *p* < 0.01; \* indicates *p*  
757 < 0.05. Spearman's correlations and *p*-values were calculated using GraphPad Prism  
758 8.4.3.

759

760 **Figure 5. Workflow of 100-cell and 10000-cell proteomic analysis using 15 multiple**  
761 **myeloma cell lines.**

762 As starting materials, 10000 or 100 cells from 15 multiple myeloma cell lines were  
763 sorted and digested in triplicate or quadruplicate. For the ISD and WinO methods,  
764 10000 or 100 cells were sorted into 1.5 mL tubes and 96-well plates, respectively.  
765 Peptides labeled with TMT reagents were combined. For the ISD method, the peptide  
766 mixture was separated into nine fractions using high-pH reverse phase fractionation.

767

768 **Figure 6. Number of peptides and proteins quantified using the ISD or WinO**  
769 **methods.**

770 The numbers of quantified peptides and proteins are shown in (A) and (B),  
771 respectively. Each bar indicates the average and standard deviations of replicate  
772 data. The proteome data obtained with the ISD and WinO methods were plotted  
773 using the UMAP (C). UMAP was performed using the umap package in R. Triangle  
774 and circle show the 100-cell and 10000-cell proteomics data, respectively. For details  
775 of sample preparation, see the legend of Figure 5.

776

777 **Figure 7. Protein identified by the WinO method.**

778 Gene ontology analysis with DAVID version 6.7  
779 (<https://david.ncifcrf.gov/summary.jsp>) was performed using 798 proteins identified  
780 from 15 multiple myeloma cell lines by the WinO method (A). Distribution of  
781 transmembrane domains (TMDs) in proteins identified with either the ISD or WinO  
782 method (B). We identified 835 and 70 TM proteins from the 15 cell lines using the  
783 ISD and WinO methods, respectively. The number of TMDs in each protein was  
784 determined from the UniProt database (<https://www.uniprot.org/>).  
785

786 **Figure 8. Application of the WinO method to single-cell proteomics.**

787 Numbers of proteins and peptides quantified using the ISD or WinO method (A). The  
788 graphs plot the average number of quantified proteins/peptides and the standard  
789 deviation of quadruplicate data. Protein levels detected from the WinO and ISD  
790 samples are compared in a volcano plot (B). Red dots indicate proteins with a  
791 significant ( $p < 0.05$ ) change of 2-fold or more. (C) compares the  $\text{Log}_{10}$  protein levels  
792 obtained by the WinO method between commonly quantified with the ISD method  
793 (239 proteins) and the uniquely quantified in the WinO method (247 proteins). Each  
794 bar shows the median. Unpaired  $t$ -tests were performed using GraphPad Prism 8.4.3.  
795

796

# Figure 1

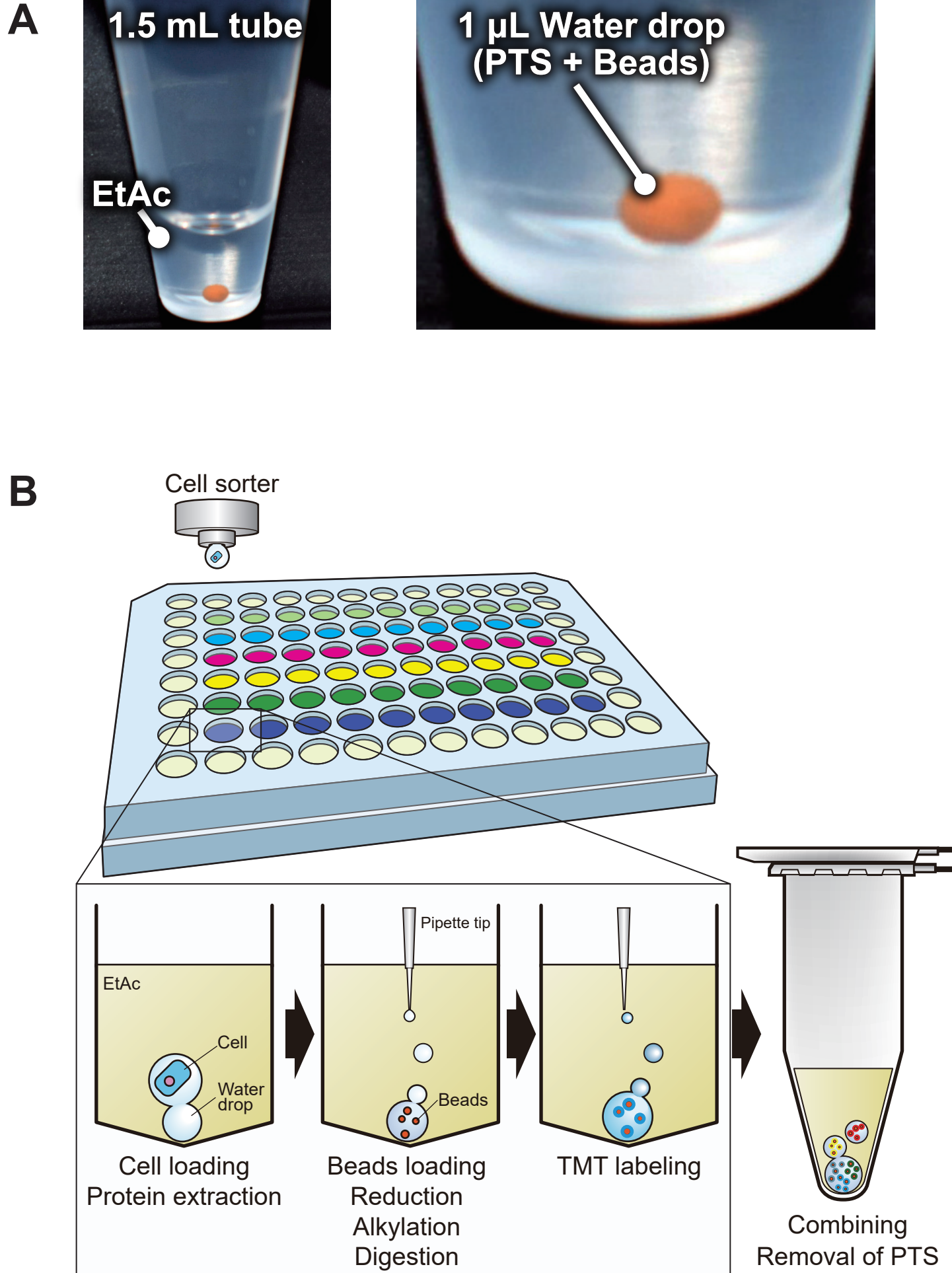
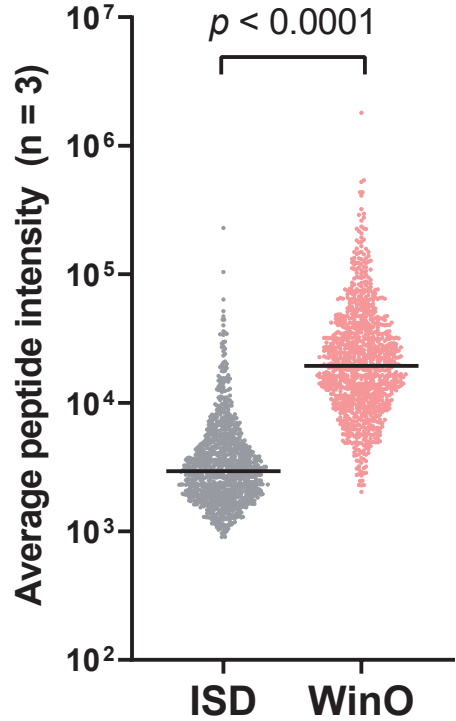
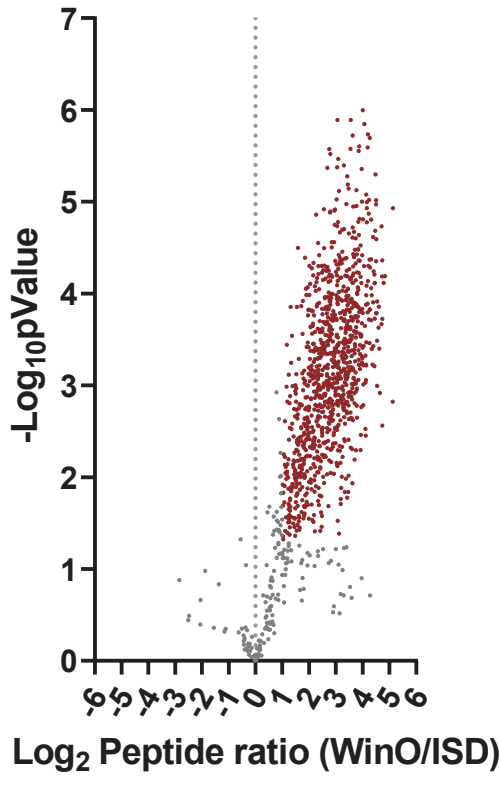


## Figure 2

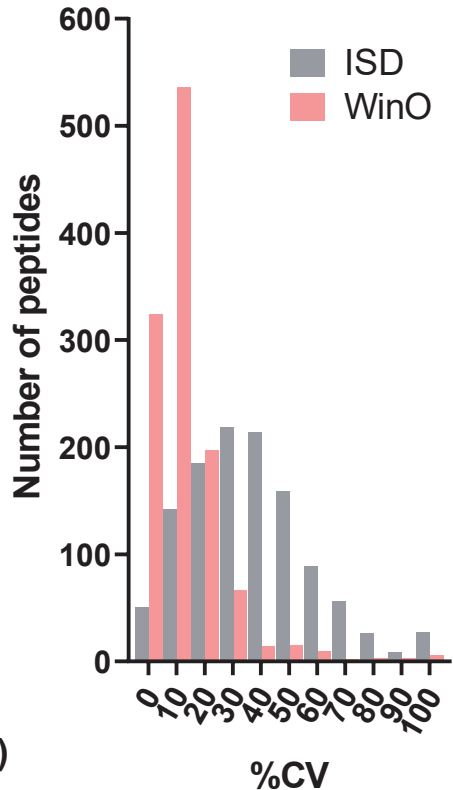
**A**



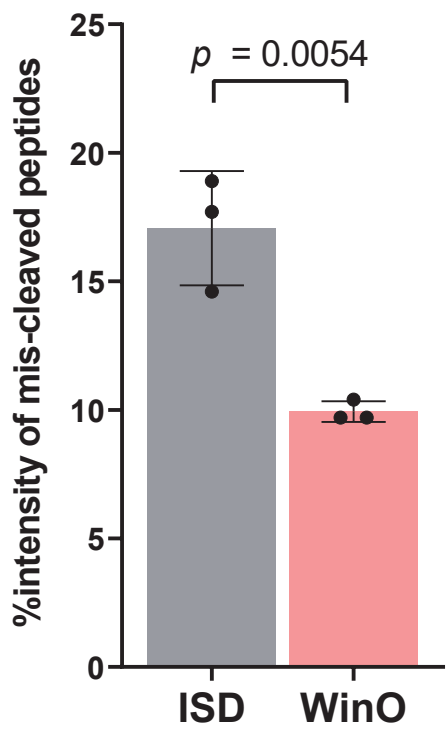
**B**



**C**



**D**



**E**

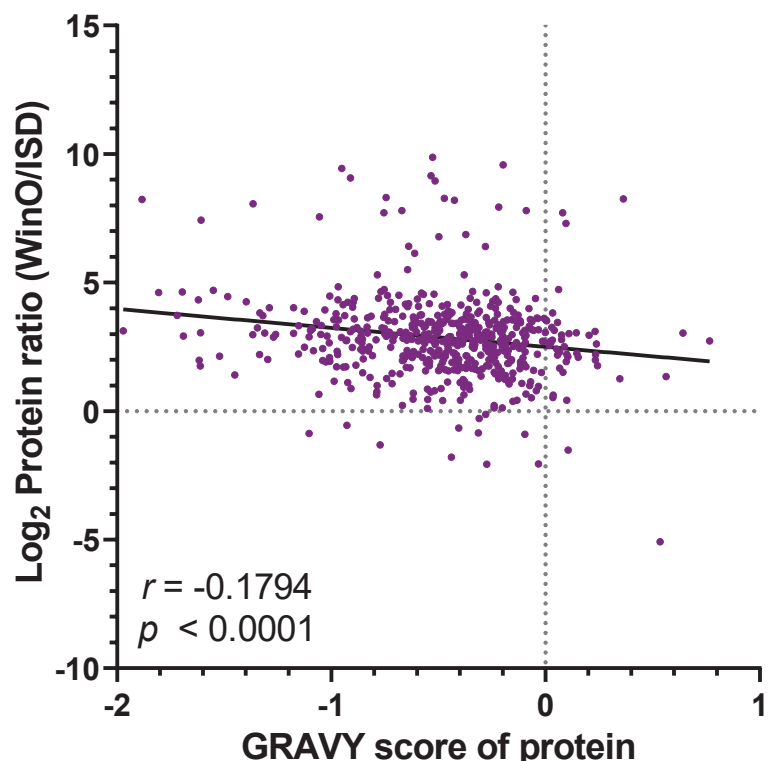
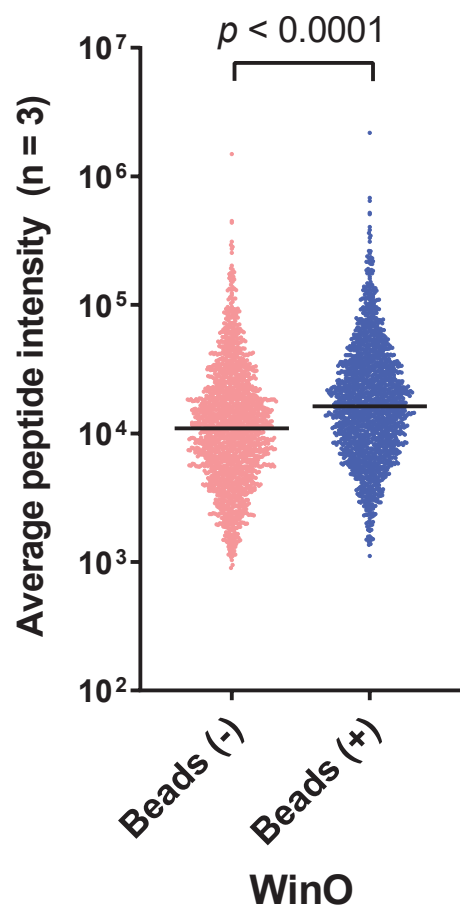
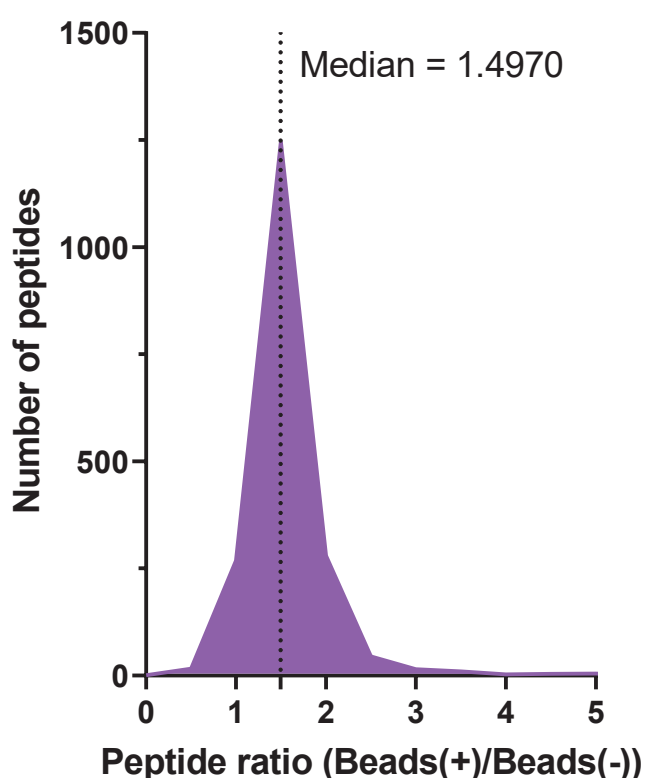


# Figure 3

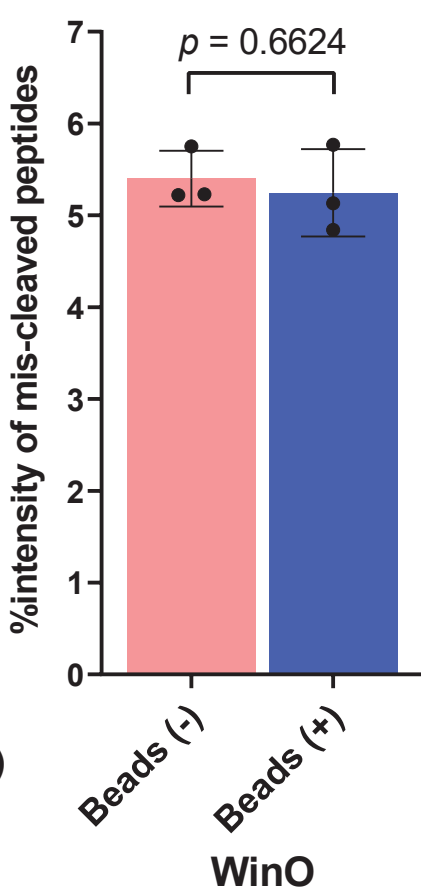
**A**



**B**



**C**



**D**

Correlation of protein levels between replicates

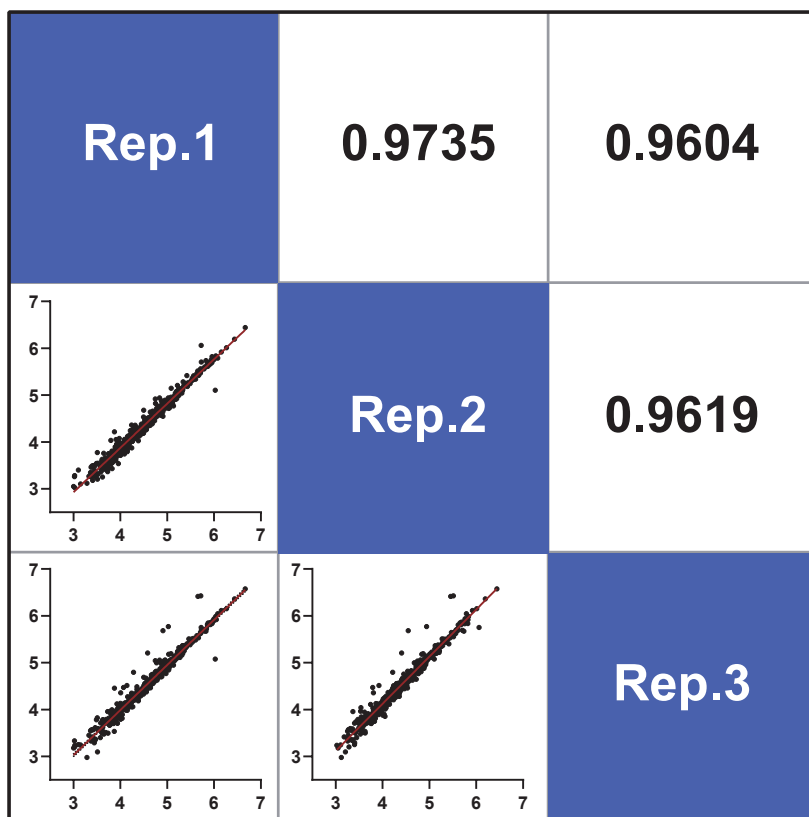
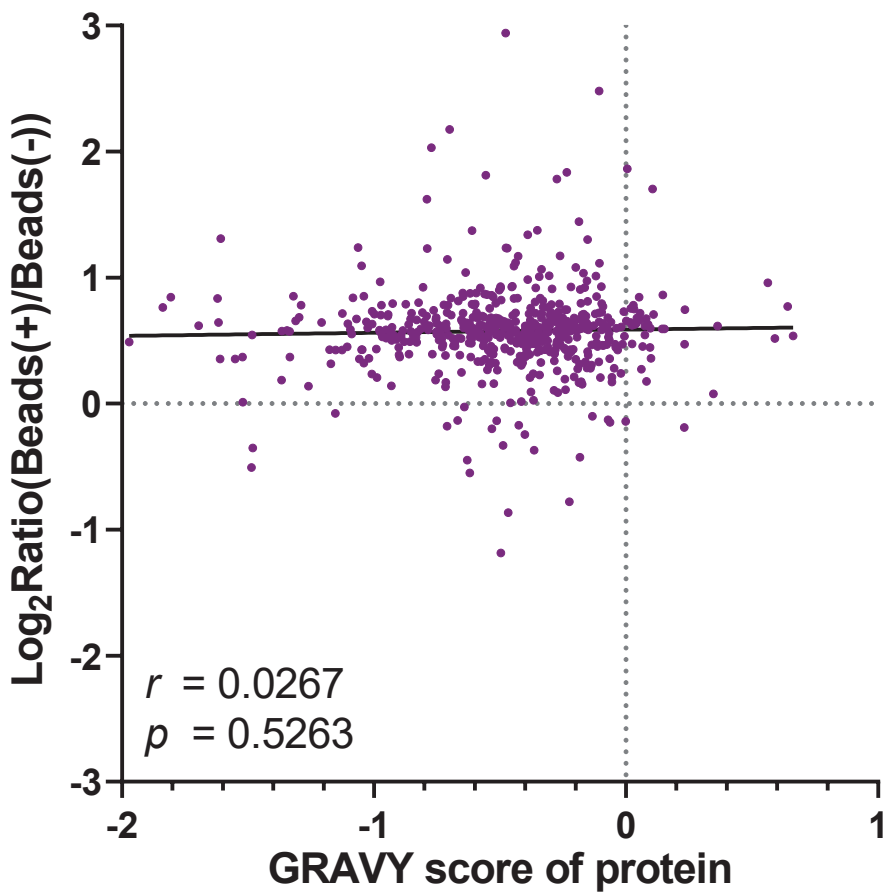


# Figure 4

**A**



**B**

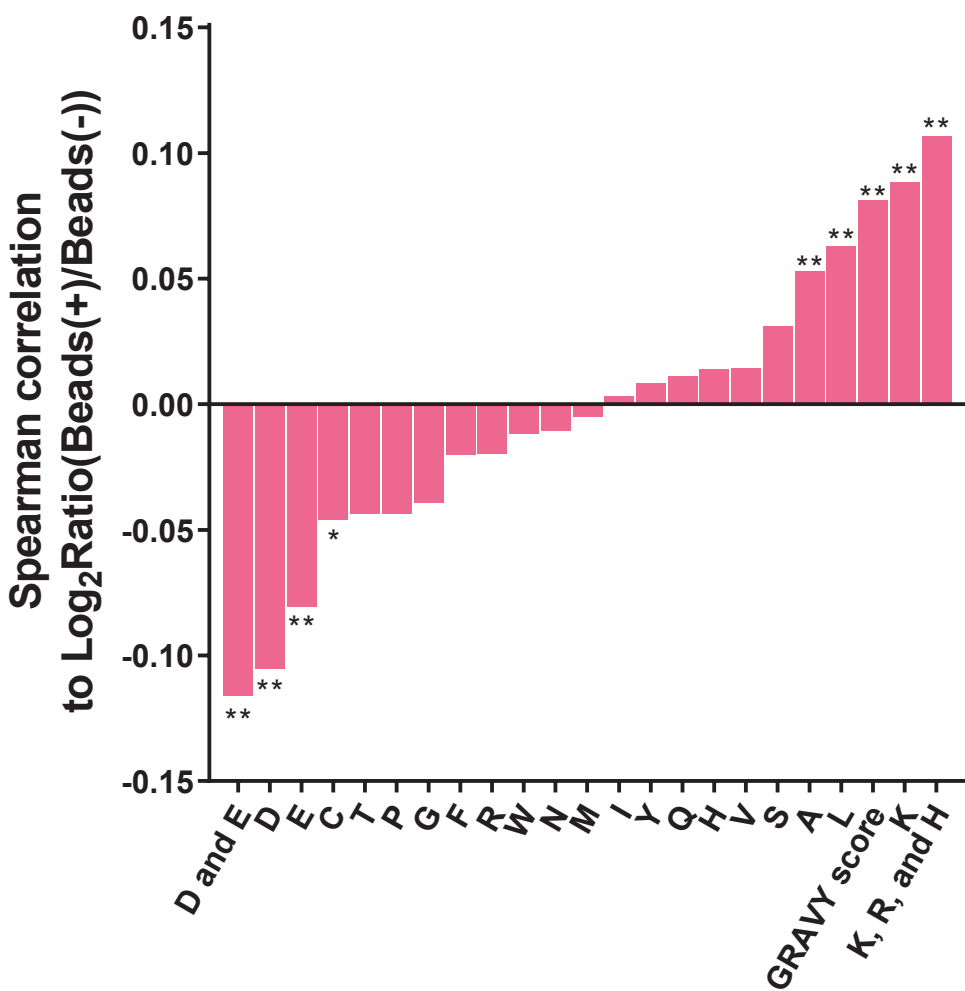


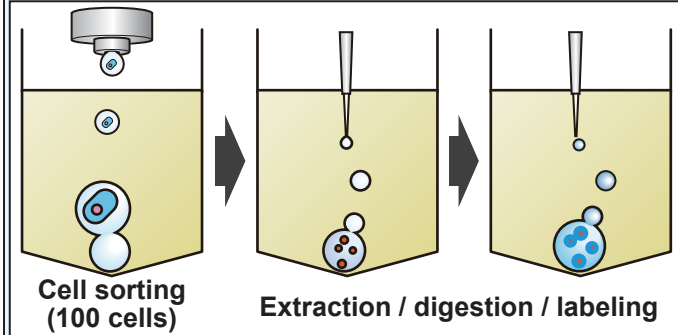
# Figure 5

## Samples

Multiple myeloma cell lines  
(n = 3 or 4)

H929	KMS-28PE
KMM-1	L363
KMS11	MM.1S
KMS-12BM	MOLP8
KMS-12PE	OPM1
KMS20	RPMI8226
KMS27	U266
KMS-28BM	

## WinO



## InSol

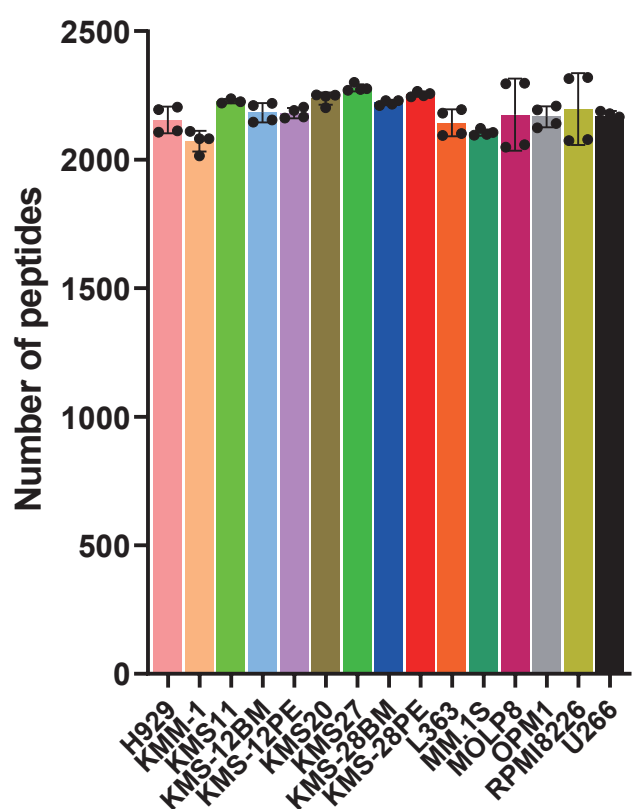
The InSol workflow is shown in five steps: 'Cell sorting (10000 cells)', 'Extraction', 'Digestion', 'Labeling', and 'Combining'. Each step is represented by a test tube containing a blue liquid. Arrows indicate the flow from the WinO steps to the InSol steps. A large grey pipette is shown on the right, dispensing liquid into the test tubes.

- Cell sorting (10000 cells)
- Extraction
- Digestion
- Labeling
- Combining
- High pH RP fractionation
- nanoLC-MS/MS

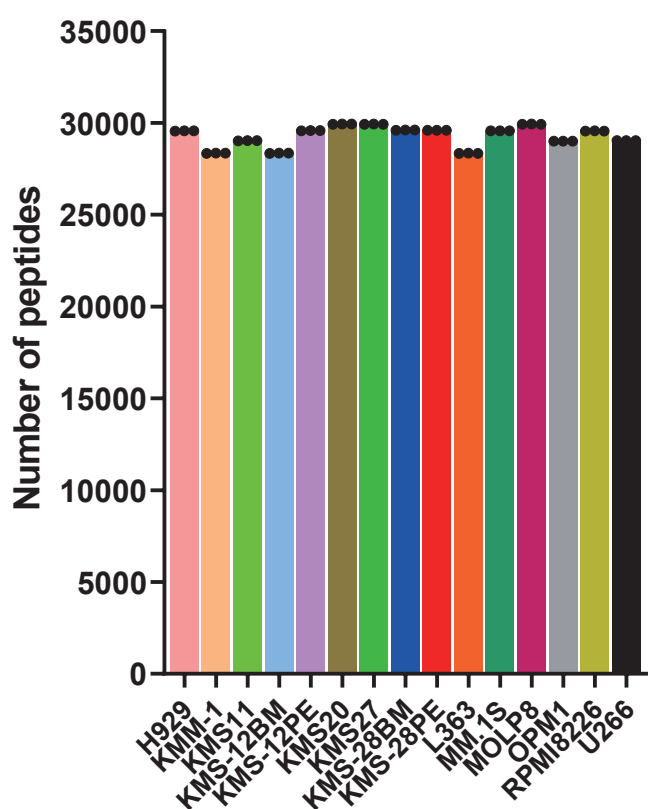
# Figure 6

**A**

**100 cells**

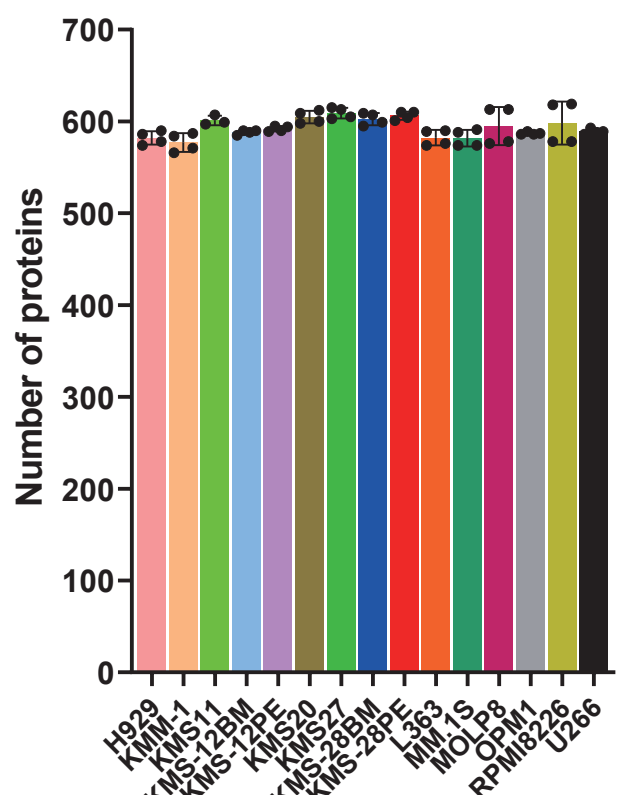


**10000 cells**



**B**

**100 cells**



**10000 cells**

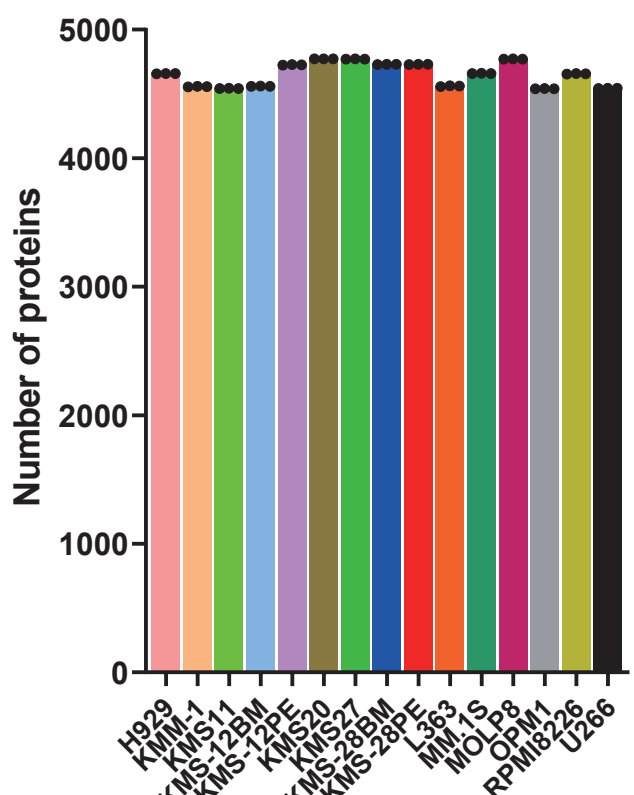


# Figure 6

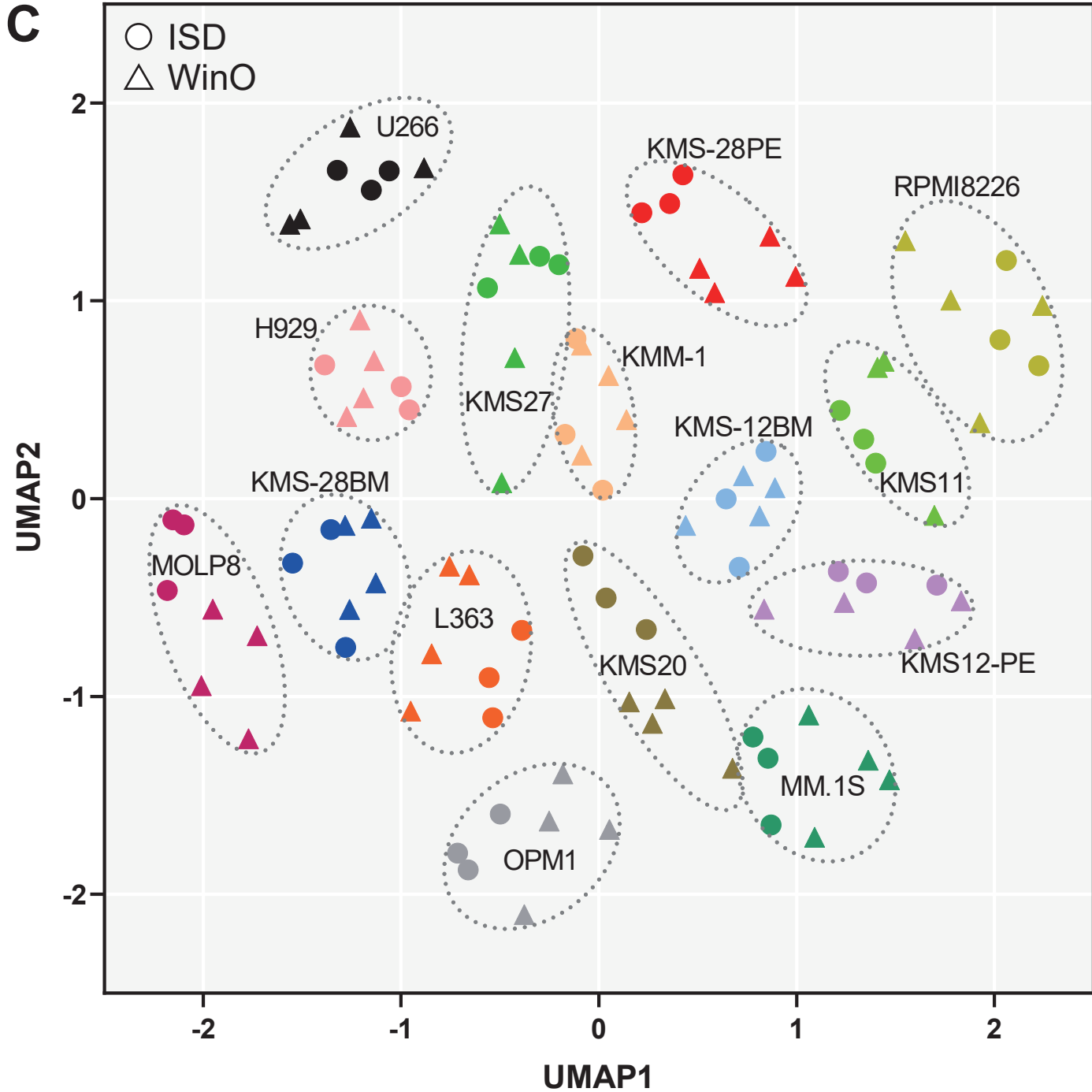
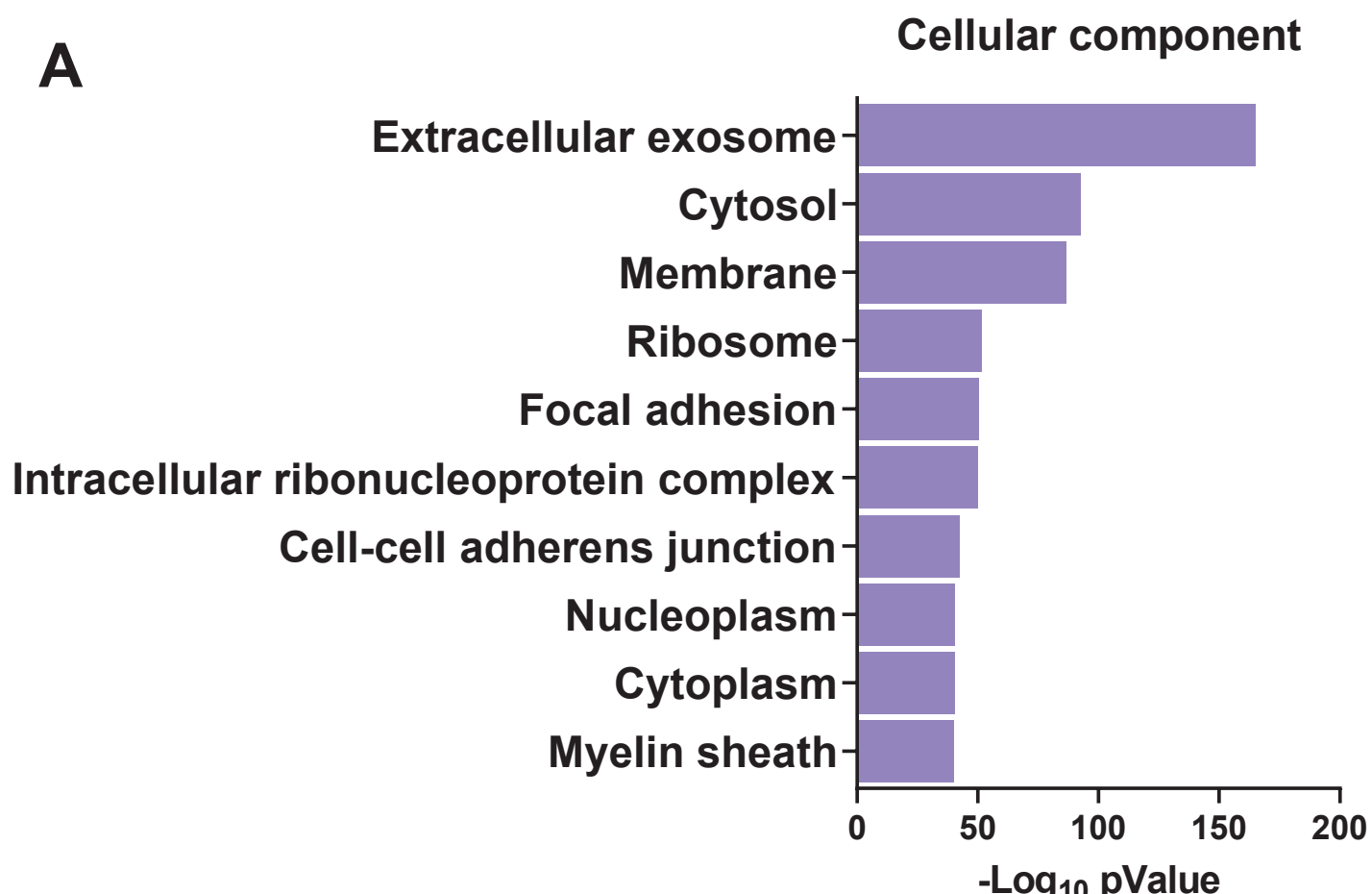


# Figure 7

A



**KEGG pathway**

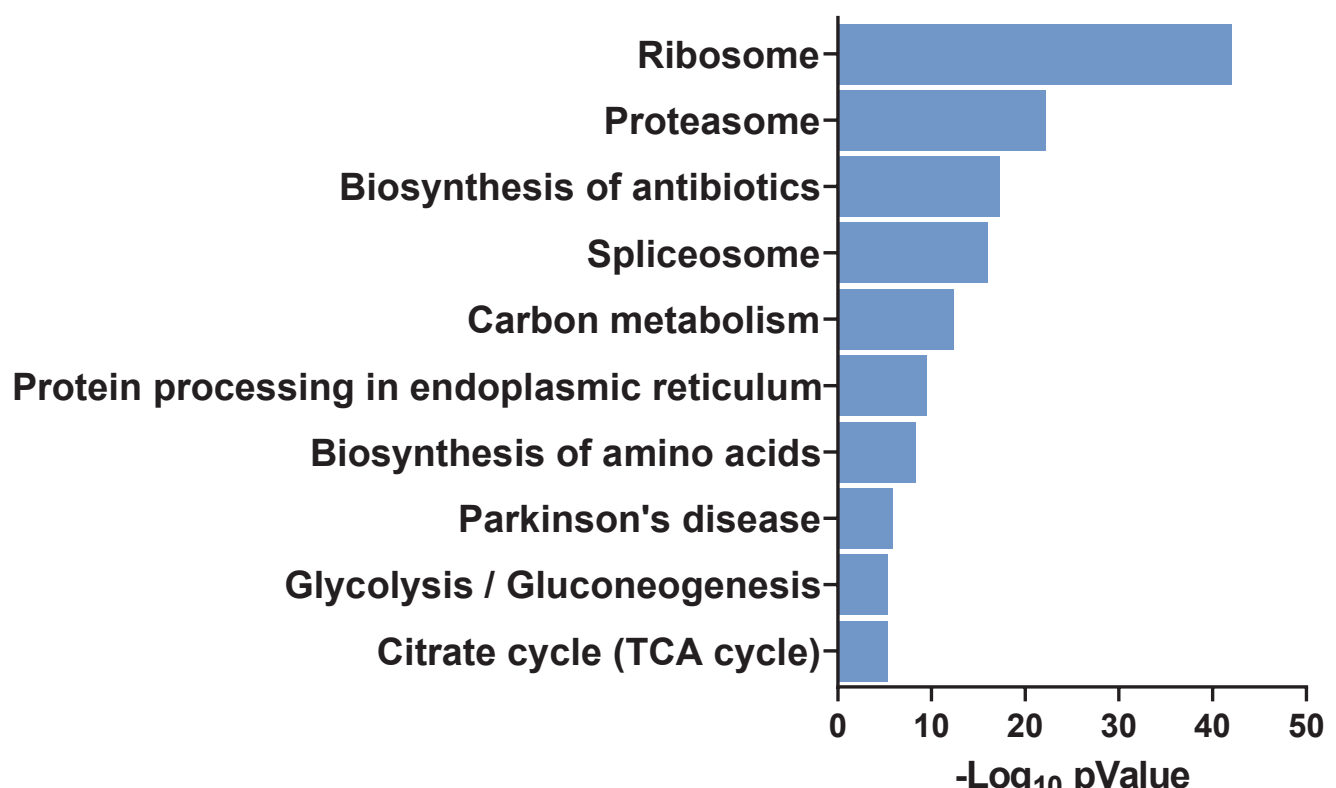


# Figure 7

**B**

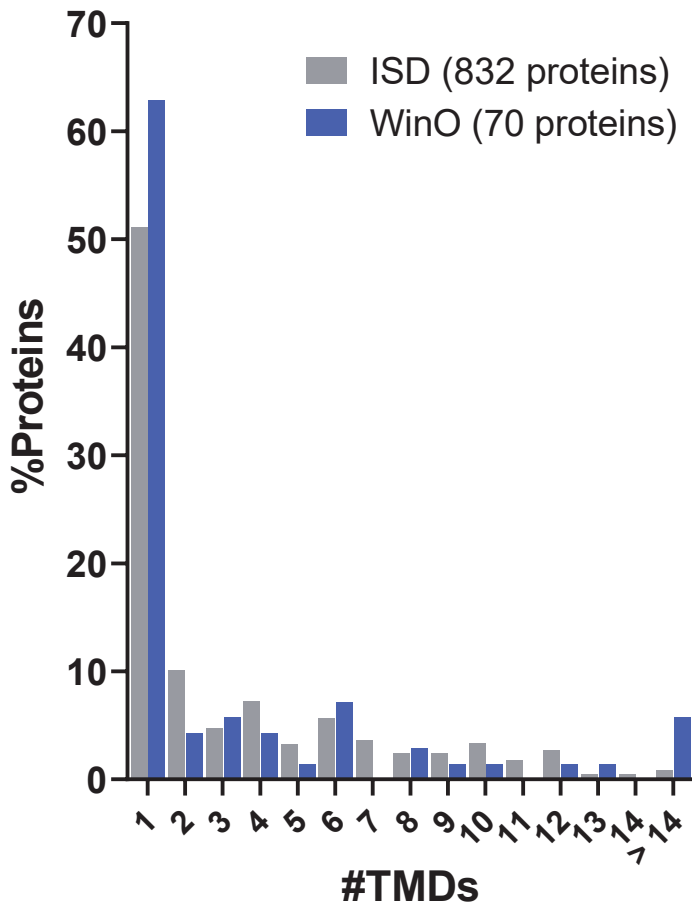
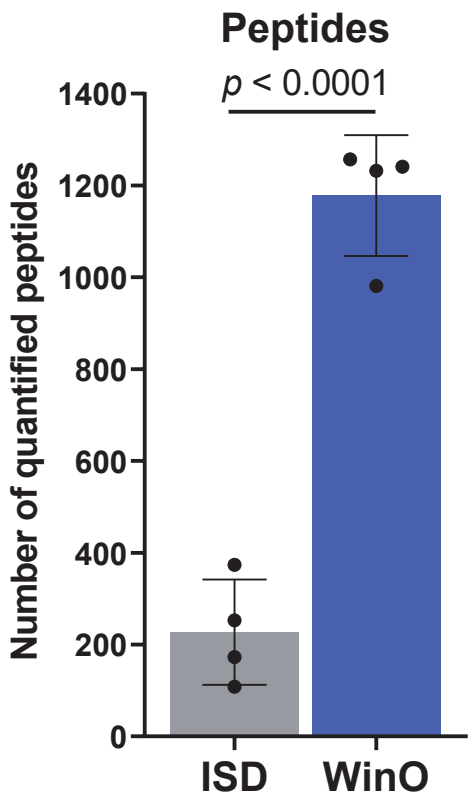
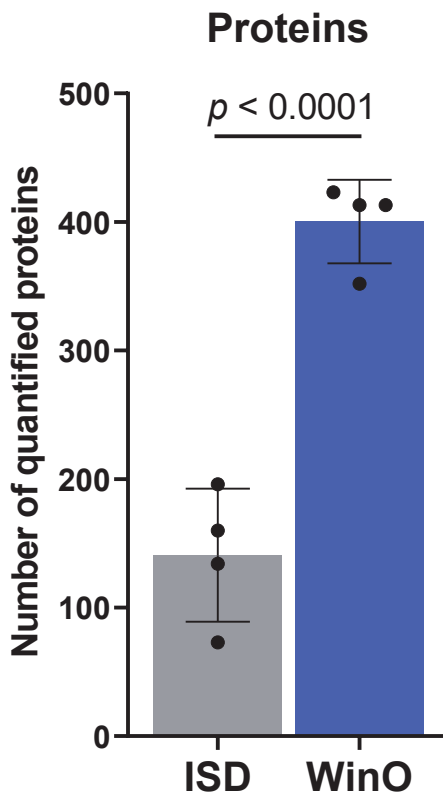


# Figure 8

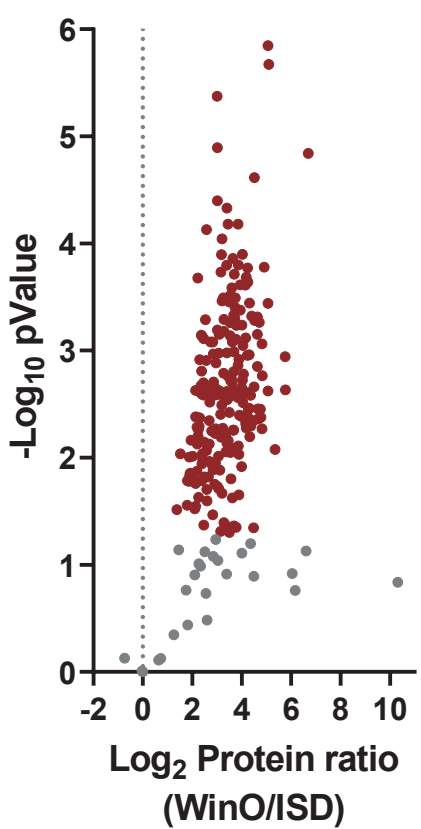
**A**



**B**



**C**



**D**

